3 RESULTS

3.1 NAADP$^+$

3.1.1 NAADP$^+$ induced different types of Ca^{2+} responses in astrocytes

It was tested whether extracellularly applied $NAADP^+$ induced Ca^{2+} signaling in cortical astrocytes in acute brain slices of 10–14-day old mice. By an appropriate protocol, the Ca^{2+} sensor Fluo-4-acetoxymethylester was preferentially loaded into astrocytes [285]. Superfusion with $NAADP^+$ (5 μM, duration of application 2–3 minutes) triggered an increase in Fluo-4 fluorescence, reflecting the change $[Ca^{2+}]_i$ in astrocytes (Fig. 7). The time course of the response showed considerable variations; single, transient responses, oscillations, a sustained elevated level, and oscillations followed by an elevated level were observed (n = 74 slices, ∅ cell number per slice = 21 ± 10; Fig. 7, *A* (*bottom*) and *B*). Generally, the Ca^{2+} responses already declined with time of $NAADP^+$ application, and a specific effect of the washout was not observed. Oscillations had an average frequency of 1.9 ± 0.7 transients per minute (for analysis: 59 oscillating cells from 21 slices). There was a considerable delay of 64 s ± 17 s between the application of $NAADP^+$ to the slice and the Ca^{2+} response (n = 11 slices, ∅ cell number per slice = 18 ± 9). To estimate whether this delay exceeded the time required for the substance to simply reach the astrocytic membranes within the slice, ATP (100 μM) was applied to activate cell membrane located purinergic receptors. This led to a more rapid Ca^{2+} response with a 20 s ± 9-s delay (n = 11 slices, ∅ cell number per slice = 16 ± 7). This difference was also confirmed with experiments in which $NAADP^+$ and ATP were applied to the same slice, separated by a 10-minute washout. The $NAADP^+$ response occurred 32 s ± 3 s (n = 5 slices, ∅ cell number per slice = 69 ± 25) later as compared with the ATP response.

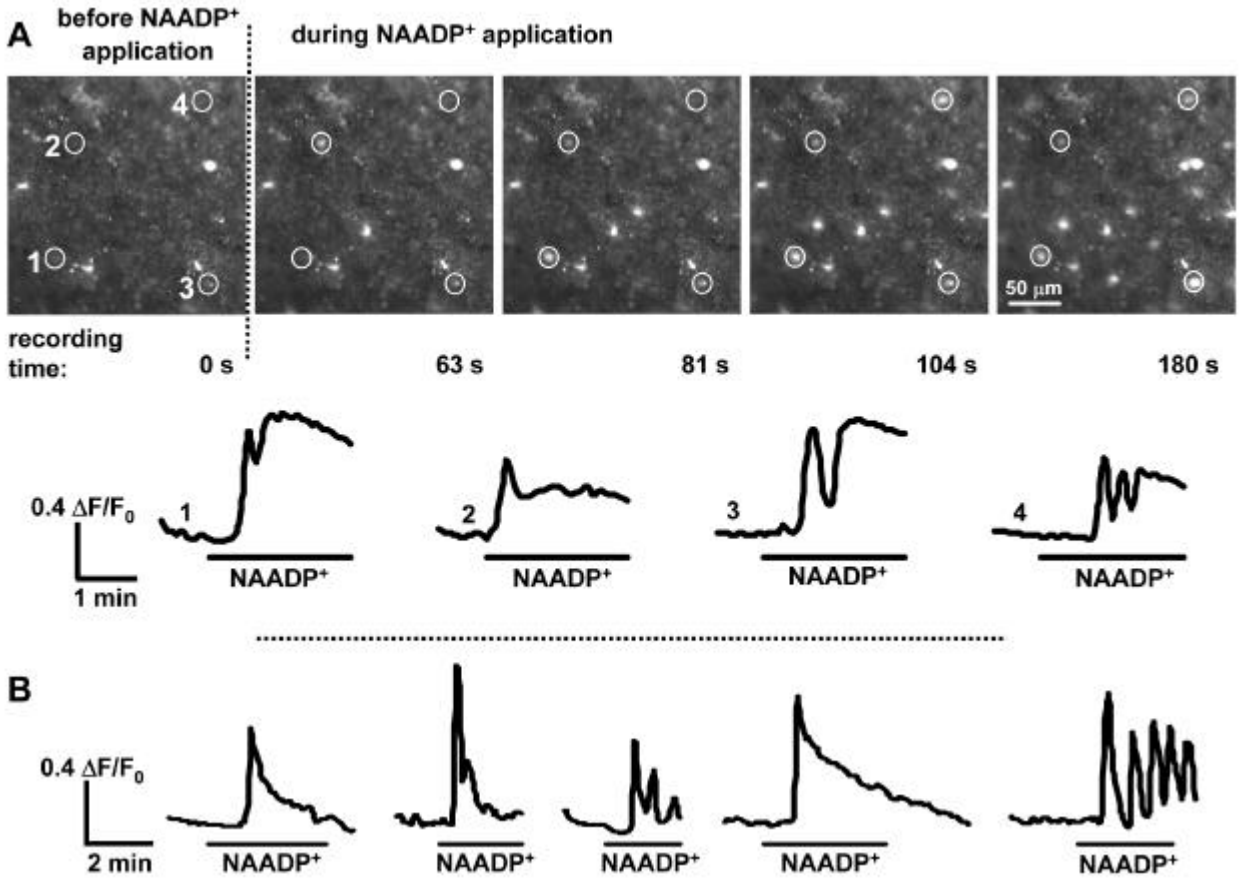

Fig. 7 NAADP$^+$ induced different types of Ca^{2+} responses in astrocytes

A, astrocytes in a neocortical slice were stained with the Ca^{2+}-sensitive dye Fluo-4. The fluorescence images are taken before and at different time points during the superfusion with $NAADP^+$ (5 µM). *Circles* label four cells, which show an increase in Fluo-4 fluorescence, and their corresponding traces are depicted *below*. The cells exhibit different response patterns. *B*, Fluo-4 fluorescence recordings from cells in different slices as additional examples of the variety of Ca^{2+} responses to $NAADP^+$ (5 µM). Responses include sustained elevated levels, single peaks followed by an elevated level, oscillations followed by an elevated level, different types of oscillations, and single transients.

3.1.2 NAADP$^+$ repetitively induced Ca^{2+} signaling in astrocytes

In non-mammalian cells, the $NAADP^+$ system desensitizes quickly, $NAADP^+$-binding is irreversible, and only one response can be triggered [277;289], whereas for mammalian cells, binding is reversible and desensitization only seems to occur at high concentrations. Therefore, repetitive signaling is possible [280;290;291]. To investigate the inactivation properties of astrocytic responses in slices, $NAADP^+$ was applied twice with a 10-minute interval (Fig. 8, *A*

and *B*). Then the cell populations, responding to the first and the second application, were compared. Almost all cells (98 ± 3%) that had responded with a Ca^{2+} increase to the first $NAADP^+$ application also responded to the second (n = 7, ∅ cell number per slice = 24 ± 9). Moreover, additional cells were found to respond to the second application, so that the total number of responsive cells increased to 117 ± 37% as compared with the first $NAADP^+$ application (Fig. 9*D*).

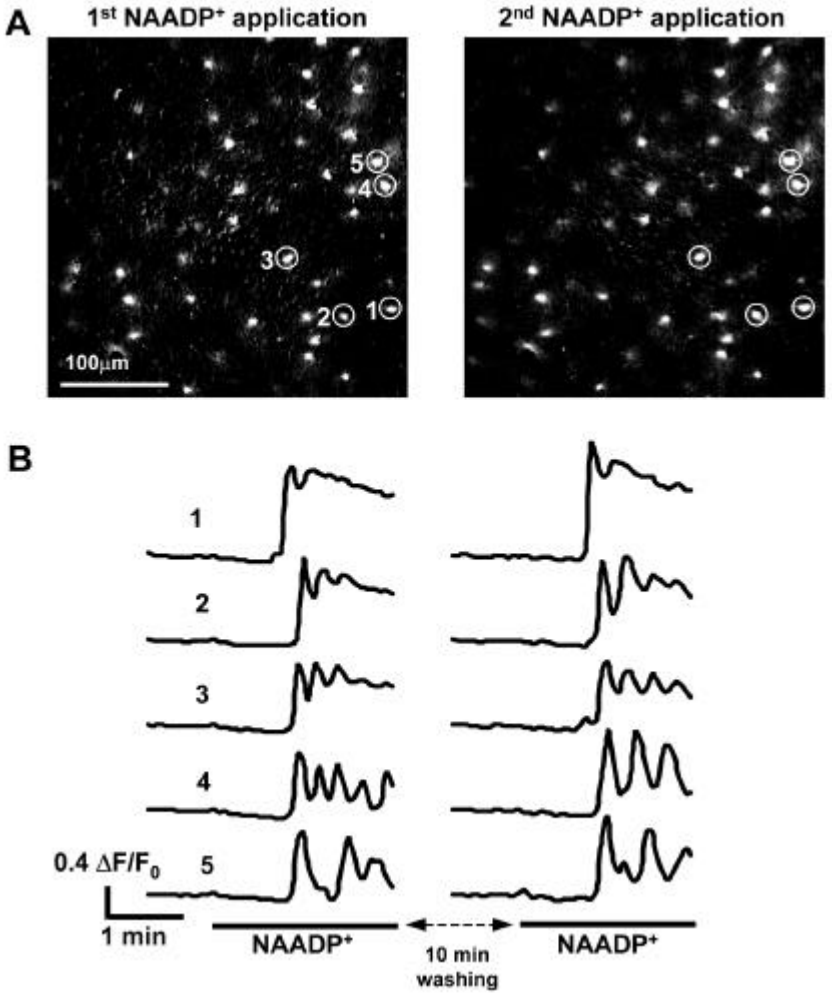

Fig. 8 $NAADP^+$ repetitively induced Ca^{2+} signaling in astrocytes

A, both fluorescence images show the same neocortical region during two subsequent $NAADP^+$ (5 µM) administrations separated by a 10-min washout. The images are subtraction images, where a control image is subtracted from an image taken during $NAADP^+$ application, so that astrocytes responding to $NAADP^+$ are bright. *B*, F/F_0 traces from five cells of this experiment are shown *below*.

As a second parameter, the "Ca^{2+} signaling activity" of the cells that reacted both times, was compared for the first and the second response. The "Ca^{2+} signaling activity" was defined as the differential F/F_0 amplitude between two consecutive images averaged over 2 minutes during $NAADP^+$ application (for details, see Materials and Methods 2.6.2). The Ca^{2+} signaling activity was on average higher for the second reaction (136 ± 37%; Fig. 9*E*). Thus, the induced signaling was comparable for both $NAADP^+$ applications, even higher during the second one. The delay from the $NAADP^+$ solution reaching the chamber to the onset of the reaction was dependent on the $NAADP^+$ concentration, since the reaction to a higher concentration (25 μM) occurred faster (11.8 s ± 6.4 s earlier; n = 13, ∅ cell number per slice = 35 ± 12).

3.1.3 $NAADP^+$ acted directly on astrocytes

To show the direct effect of $NAADP^+$ on astrocytes, purified astrocyte cultures from mouse brain were used. In these cells, similar types of Ca^{2+} responses were triggered by $NAADP^+$ (n = 7 coverslips; Fig. 9, *A* and *B*). Also in culture, $NAADP^+$-induced signaling could be repetitively elicited (n = 3 coverslips; Fig. 9*C*). In a slice preparation, indirect effects mediated by other cell types cannot be excluded. The response of the astrocytes could therefore result from substances released by other cell types in response to $NAADP^+$. To eliminate at least one factor, neuronal action potentials were blocked by tetrodotoxin (TTX) during application of $NAADP^+$. Since there is a high variability of responses to $NAADP^+$ between different slices, Ca^{2+} responses to $NAADP^+$ in the absence (internal control) and presence of TTX (1 μM) were compared in the same area of one slice, separated by a 5-minute washout and a 5-minute TTX preincubation. TTX did not significantly reduce the number of responding cells (96 ± 19%; n = 5, ∅ cell number per slice = 23 ± 6). Of the cells, which still responded, 90 ± 16% had reacted again, whereas 6 ± 8% reacted in addition (Fig. 9*D*). However, the average Ca^{2+} signaling activity was reduced to 78 ± 24% ($p < 0.05$; Fig. 9*E*).

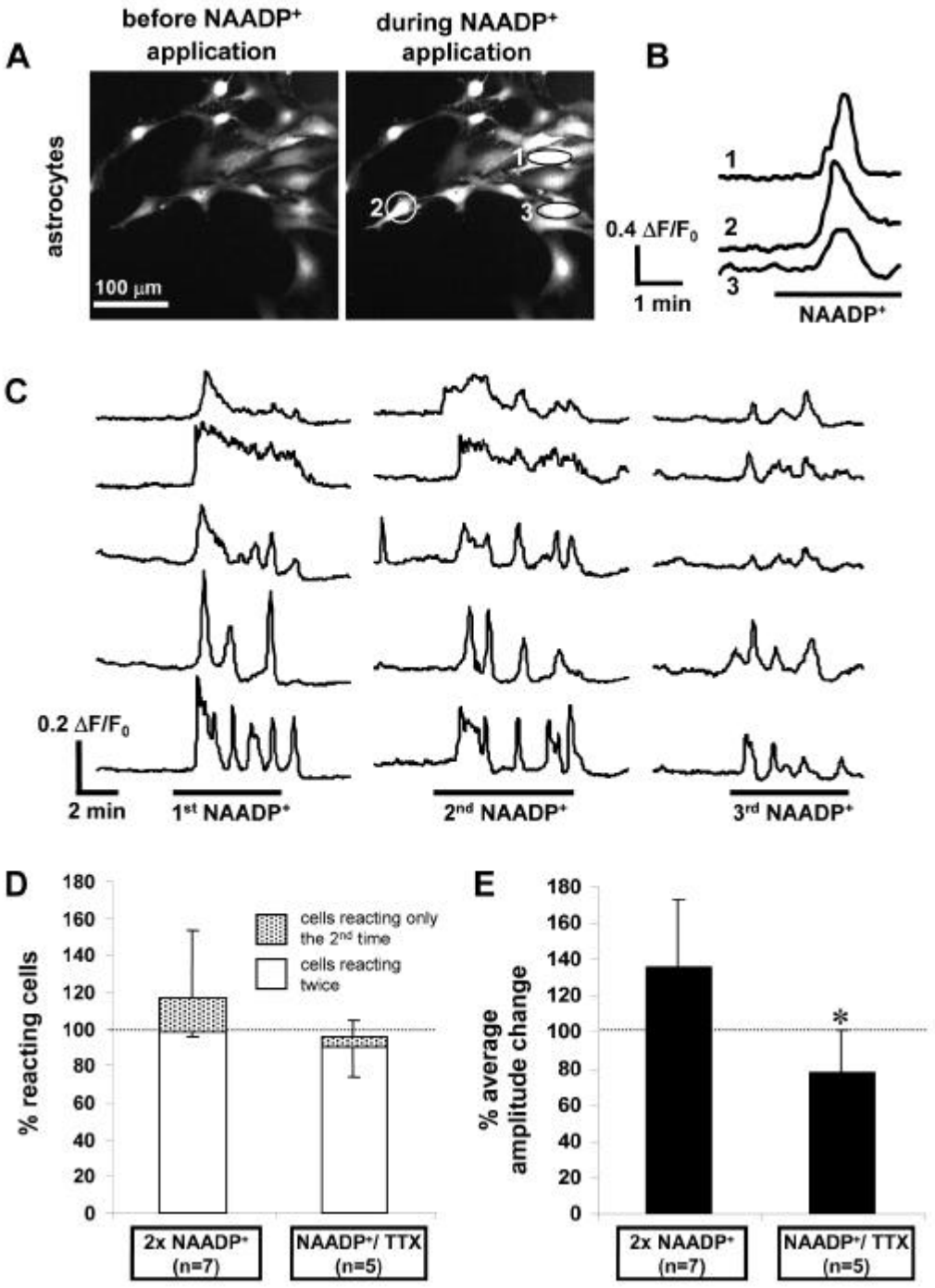

Fig. 9 NAADP$^+$ acted directly on astrocytes

A shows Fluo-4 loaded cultured astrocytes. The *first image* was taken before; the *second image* was taken during perfusion with NAADP$^+$ (5 μM). *B*, F/F_0 traces are shown from cells marked in *A*. *C*, F/F_0 traces from five different astrocytes in culture superfused three times with NAADP$^+$ (5 μM); cultured astrocytes also respond to repetitive superfusion with NAADP$^+$. *D, bar graph* on the *left* compares the number of astrocytes responding with a $[Ca^{2+}]_i$ increase to two subsequent NAADP$^+$ applications separated by 10 min (*left*). The number of reacting cells from the

first application is defined as 100% and the relative number of cells responding to the second application is given in the *graph*. The *graph* shows averages of several experiments and *n* indicates the number of brain slices from which data were obtained for this and for the figures to follow. The *right bar* shows a similar type of experiment, in which TTX (1μM) was present during the second application. TTX was applied 5 min prior to the second $NAADP^+$ application. *E*, *bar graph* comparing the average amplitude change of the fluorescence intensity of cells during two subsequent $NAADP^+$ applications (for details, see Materials and Methods). Only those cells were selected that reacted to both $NAADP^+$ applications. The *left bar* corresponds to two control $NAADP^+$ applications, and the *right bar* to a control followed by a $NAADP^+$ application in the presence of TTX. *, $p < 0.05$; **, $p < 0.005$.

3.1.4 $NAADP^+$ precursors also induced Ca^{2+} signaling in astrocytes

Application of the two precursors of $NAADP^+$, $NADP^+$ and NAAD, induced similar Ca^{2+} elevations as observed for $NAADP^+$ (Fig. 10, *A* and *B*). First, $NAADP^+$ (5 μM) was applied and then, after a 10-minute washout, $NADP^+$ (5 μM) or NAAD (5 μM). All cells that reacted to $NAADP^+$ reacted to $NADP^+$ (100 ± 1%; $n = 9$, ∅ cell number per slice = 57 ± 18; Fig. 10*C*). The same applied to NAAD (98 ± 2%; $n = 9$, ∅ cell number per slice = 44 ± 14; Fig. 10*C*). The responses to $NADP^+$ and NAAD occurred with a similar delay as observed for $NAADP^+$ (Fig. 10, *A* and *B*).

3.1.5 $NAADP^+$-induced Ca^{2+} signaling depended on functional connexin hemichannels/gap junctions and extracellular Ca^{2+}

It was investigated whether connexin hemichannels may serve as an entry route for $NAADP^+$ into the cytoplasm. For this reason, connexin hemichannels (and gap junctions) were blocked during the application of $NAADP^+$ to observe whether this would reduce the response to $NAADP^+$. After the first $NAADP^+$ application, it was washed for 5 minutes followed by superfusion with the gap junction blocker carbenoxolone (100 μM, 5 minutes). $NAADP^+$ was then applied in the presence of carbenoxolone. Only 54 ± 34% of the cells responded in comparison to a previous control application. 47 ± 24% of the cells had reacted already before, and 7 ± 18% reacted additionally ($p < 0.005$; $n = 12$, ∅ cell number per slice = 20 ± 7; Fig. 11*A*). The average activity was also reduced to 71 ± 38% during blockage of connexin hemichannels ($p < 0.05$; $n = 6$, ∅ cell number per slice = 20 ± 9; Fig. 11*B*).

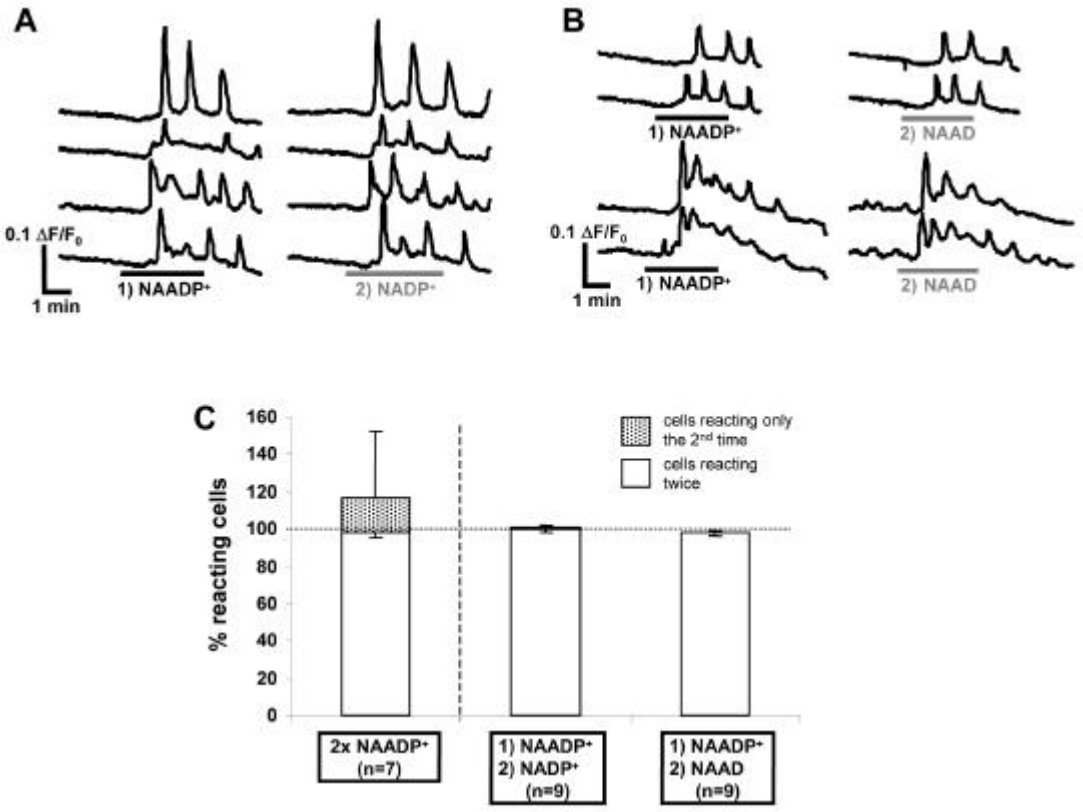

Fig. 10 Precursors of NAADP$^+$ induced Ca^{2+} signaling

A, F/F_0 traces of four cells from the same slice showing a similar response pattern to $NAADP^+$ (5µM) and to $NADP^+$ (5µM). *B*, F/F_0 traces of four cells from two different slices showing a similar response pattern to $NAADP^+$ and to NAAD (5µM). *C*, the *bar graph* compares the number of astrocytes responding with a $[Ca^{2+}]_i$ increase to either two subsequent $NAADP^+$ applications or an $NAADP^+$ application followed by a $NADP^+$ or NAAD application similar as described in the legend to Fig. 9*D*.

3.1.6 Ca^{2+} influx is a component of $NAADP^+$-induced Ca^{2+} signals

To analyze the mechanism of the $NAADP^+$-triggered response, it was tried to distinguish between Ca^{2+} influx and release from internal stores. Therefore, the effects of $NAADP^+$ application in normal and nominally Ca^{2+}-free bath solution were compared. A control response in normal bath solution was recorded first and then the $NAADP^+$ was washed out with control solution for 5 minutes. Afterwards, it was switched to a nominally Ca^{2+}-free buffer for 5 minutes and $NAADP^+$ was applied again, still in the absence of Ca^{2+} in the bath. The number of cells per slice responding to $NAADP^+$ with a Ca^{2+} increase was reduced to 48 ± 38% as compared with the control. Almost all of these cells had responded in the control solution (47 ± 37%), and nearly

none (1 ± 2%) responded only in the Ca^{2+}-free solution ($p < 0.005$; $n = 8$, ∅ cell number per slice = 24 ± 10; Fig. 11*A*). The lack of extracellular Ca^{2+} also reduced the Ca^{2+} signaling activity to 61 ± 23% compared with the original reaction ($p < 0.005$; Fig. 11*B*). Furthermore, only transient Ca^{2+} responses were observed and never an increase to a sustained level.

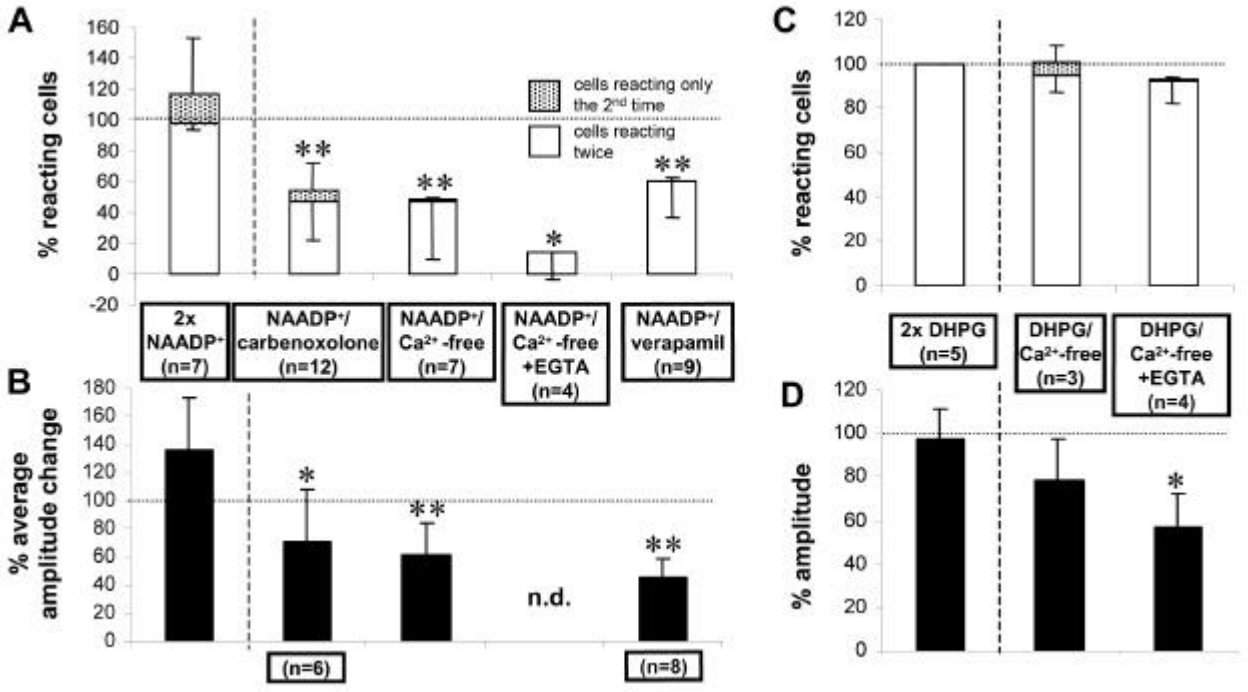

Fig. 11 Pharmacology of $NAADP^+$ induced Ca^{2+} signaling in astrocytes I

A, similar as described in the legend to Fig. 9, the populations of reacting cells were compared between two control $NAADP^+$ applications (2× $NAADP^+$), between a control $NAADP^+$ application and a $NAADP^+$ application combined with carbenoxolone (100 μM, 5-min preincubation), nominal Ca^{2+} free buffer (5-min preincubation), Ca^{2+} free buffer containing EGTA (1 mM, 2-3-min preincubation), or the L-type Ca^{2+} channel blocker verapamil (100 μM, 15-min preincubation). *B*, the average amplitude change of the fluorescence intensity was obtained as described in the legend to Fig. 9. *C* and *D*, DHPG (20 μM) was applied using the same experimental paradigm as described for $NAADP^+$ application in *A* and *B*. Cell populations were compared in *C*. The peak amplitudes of the DHPG responses are given in *D*. Control DHPG applications were compared to DHPG applications combined with nominal Ca^{2+} free buffer (5-min preincubation), Ca^{2+} free buffer containing EGTA (1 mM, 2-3 min preincubation). *, $p < 0.05$; **, $p < 0.005$.

To test whether residual extracellular Ca^{2+} might have accounted for the remaining signals, the experiment was repeated with EGTA-containing Ca^{2+}-free buffer (1 mM, 2–3-minute preincubation after a 7–8-min washout with normal bath solution) and far fewer cells were found

responding to $NAADP^+$ (14 ± 17%, $p < 0.05$) than in a previous Ca^{2+}-containing control reaction (n = 4, ∅ cell number per slice = 11 ± 3). The cells that still responded to $NAADP^+$, had also responded in the control solution (Fig. 11*A*). To test whether the Ca^{2+}-free or EGTA/Ca^{2+}-free treatment would generally affect the filling state of the intracellular stores, $NAADP^+$ was substituted with the metabotropic GluR group I agonist DHPG (20 μM), which triggers release from intracellular stores, using the same experimental paradigm. In the nominally Ca^{2+}-free buffer, the average number of cells responding to DHPG was the same as in the presence of Ca^{2+} (100 ± 3%; n = 3, ∅ cell number per slice = 36 ± 14). 94 ± 8% were the same cells and 6 ± 7% reacted additionally (Fig. 11*C*). However, their amplitude was in average reduced to 78 ± 19% (Fig. 11*D*). In EGTA containing Ca^{2+}-free buffer, the number of DHPG-responsive cells was slightly reduced to 92 ± 10% (Fig. 11*C*). The amplitude of the astrocytes, which still responded, was more strongly affected (57 ± 16% of the internal control, $p < 0.05$; n = 4, ∅ cell number per slice = 49 ± 7; Fig. 11*D*). Two consecutive applications of DHPG in Ca^{2+}-containing solution resulted in responses of the same population of astrocytes (Fig. 11*C*), and the average amplitude of the second response was only slightly reduced to 97 ± 14% (n = 5, ∅ cell number per slice = 33 ± 8; Fig. 11*D*). When comparing responses to DHPG and $NAADP^+$, it is evident that the $NAADP^+$-triggered Ca^{2+} signaling was more sensitive to the omission of extracellular Ca^{2+}.

Since it was reported that L-type Ca^{2+} channel blockers interfere with $NAADP^+$-induced Ca^{2+} signaling, the effect of the L-type Ca^{2+} channel blocker verapamil on $NAADP^+$-induced Ca^{2+} signaling was tested. Verapamil (100 μM, 15-minute preincubation) reduced the $NAADP^+$-responding cell population to 60 ± 23% ($p < 0.005$; Fig. 11*A*) and their average activity to 45 ± 14 % ($p < 0.005$; n = 9, ∅ cell number per slice = 29 ± 11; Fig. 11*B*), similarly to the nominally Ca^{2+}-free condition.

3.1.7 $NAADP^+$-induced Ca^{2+} signaling depended on the integrity of intracellular Ca^{2+} stores

To investigate whether intracellular thapsigargin-sensitive stores are involved in the $NAADP^+$-induced Ca^{2+} responses in astrocytes, a control $NAADP^+$ application was compared to an application after 12–20-minutes of superfusion with thapsigargin (1 μM), which leads to a depletion of endoplasmic reticulum Ca^{2+} stores. This treatment nearly completely abolished Ca^{2+}

responses to $NAADP^+$ application (5 ± 11% cells of internal control, $p < 0.005$; *n* = 5, ∅ cell number per slice = 17 ± 9; Fig. 12*A*). Similarly, blocking IP_3 receptors with 2-aminoethoxydiphenylborane (2-APB; 100 µM, 10-minute preincubation) reduced the number of cells responding to $NAADP^+$ very strongly, namely to 10 ± 15% as compared to a control response in normal bath solution ($p < 0.05$; n = 4, ∅ cell number per slice = 12 ± 3; Fig. 12*A*).

$NAADP^+$ is thought to act on receptors located on lysosomes and to release Ca^{2+} from these organelles. Therefore, lysosomes were disrupted by incubation with GPN, a cathepsin C substrate. Cathepsin C is located exclusively in lysosomes and the GPN degradation products lead to osmotic swelling followed by disruption of lysosomes. Perfusion with GPN (200 µM) itself induced transient Ca^{2+} signaling in astrocytes in brain slices (*n* = 4, ∅ cell number per slice = 18 ±6; Fig. 12*B*). When $NAADP^+$ was applied in the presence of GPN after a 4-minute GPN preincubation, the average number of $NAADP^+$-responsive cells was reduced to 25 ± 39% in comparison with the internal control $NAADP^+$ application ($p < 0.005$; *n* = 14, ∅ cell number per slice = 26 ± 10; Fig. 12*A*). To explore a possible interference of GPN with intracellular Ca^{2+} release from thapsigargin-sensitive stores, it was stimulated with the metabotropic glutamate receptor type I agonist tACPD (50 µM). In comparison with the effect on the response to $NAADP^+$, GPN had a modest effect on the response to tACPD. It reduced the average number of reacting cells to 65 ± 34% ($p < 0.05$; *n* = 4, ∅ cell number per slice = 22 ± 8) as compared to the internal control (Fig. 12*C*). GPN furthermore reduced the Ca^{2+} signaling amplitude of cells to 58 ± 20% ($p < 0.05$; *n* = 3, ∅ cell number per slice = 18 ± 3; Fig. 12*D*). This effect was not due to run down of tACPD-triggered Ca^{2+}-signaling; 100% of cells responded to a second application of tACPD (*n* = 6, ∅ cell number per slice = 35 ± 10; Fig. 12*C*), and the amplitude of the second reaction was in average only slightly reduced (94 ± 21% of the first response; Fig. 12*D*).

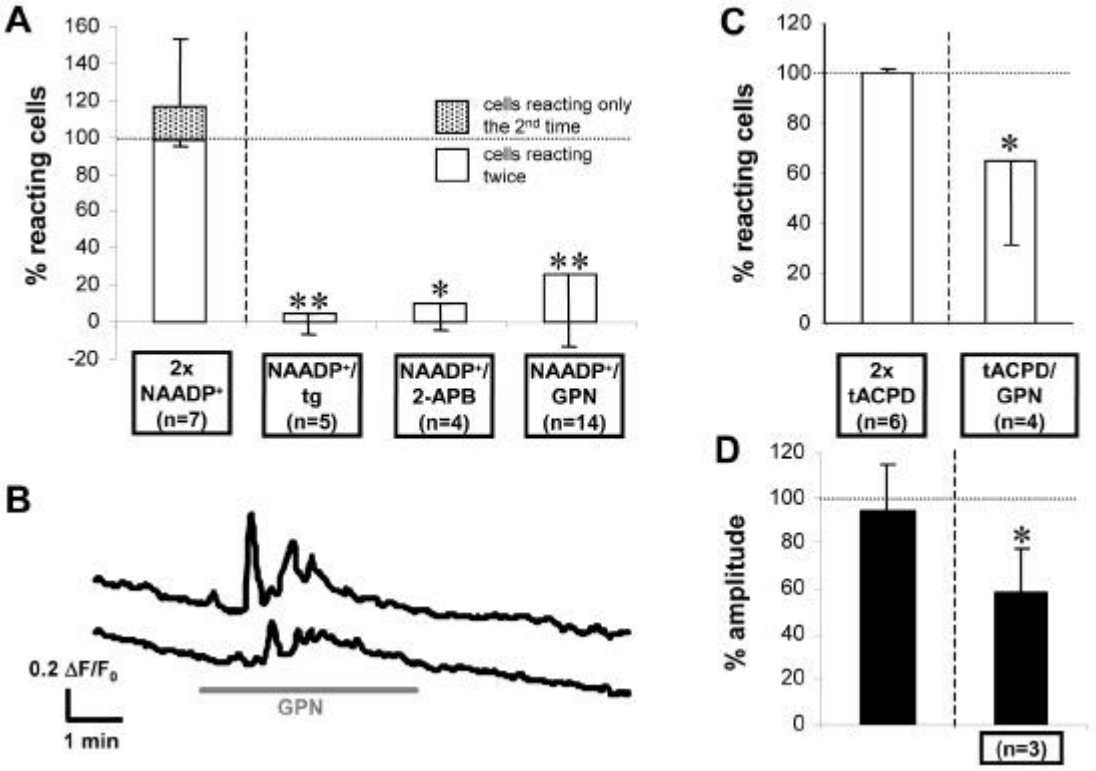

Fig. 12 Pharmacology of NAADP$^+$-induced Ca^{2+} signaling in astrocytes II

A, as described in the legend to Fig. 9, the number of cells responding to a NAADP$^+$ application was compared to a NAADP$^+$ application in the presence of thapsigargin (tg, 1 μM, 12-20-min preincubation), the IP_3 receptor blocker 2-APB (100 μM, 10-min preincubation) and an agent to disrupt lysosomes, GPN (200 μM, 4-min preincubation). *B*, F/F_0 traces of Fluo-4 fluorescence recording from astrocytes during application of GPN (200 μM) indicating that GPN triggered an increase in $[Ca^{2+}]_i$. *C* and *D*, the number of responding cells and the peak amplitude of the fluorescence intensity are given similar as described in the legend to Fig. 9. Compared were two control tACPD (50 μM) applications (*left*) and a control tACPD application with a tACPD application in the presence of GPN (*right*). *, $p < 0.05$; **, $p < 0.005$.

3.1.8 Purinergic and adenosine-mediated contribution to the NAADP$^+$-induced signal

Extracellularly applied NAADP$^+$ could potentially activate purinergic signaling either by degradation products or by direct interaction with purinergic receptors. To address this question, two different purinergic receptor blockers (suramin and PPADS) were used; however, in control experiments with ATP, both did not have a strong effect in brain slices. Therefore, another

approach was applied to study the interaction between purinergic and $NAADP^+$-induced signaling.

Purinergic receptors were desensitized by continuous ATP application (100 µM). Subsequently, it was waited 3–5 minutes until the Ca^{2+} concentration returned to base-line level, and then $NAADP^+$ was applied in the presence of ATP. In most experiments, $NAADP^+$ triggered a Ca^{2+} response, albeit reduced (*n* = 29; Fig. 13, *B* and *C*). As control, tACPD (50 µM), whose signaling pathway is at least initially different from that of ATP, was used and applied in the presence of ATP. The Ca^{2+} signal to tACPD in the presence of ATP was similarly reduced as that of $NAADP^+$ in comparison to a first control application without ATP (*n* = 8; Fig. 13, *A* and *C*).

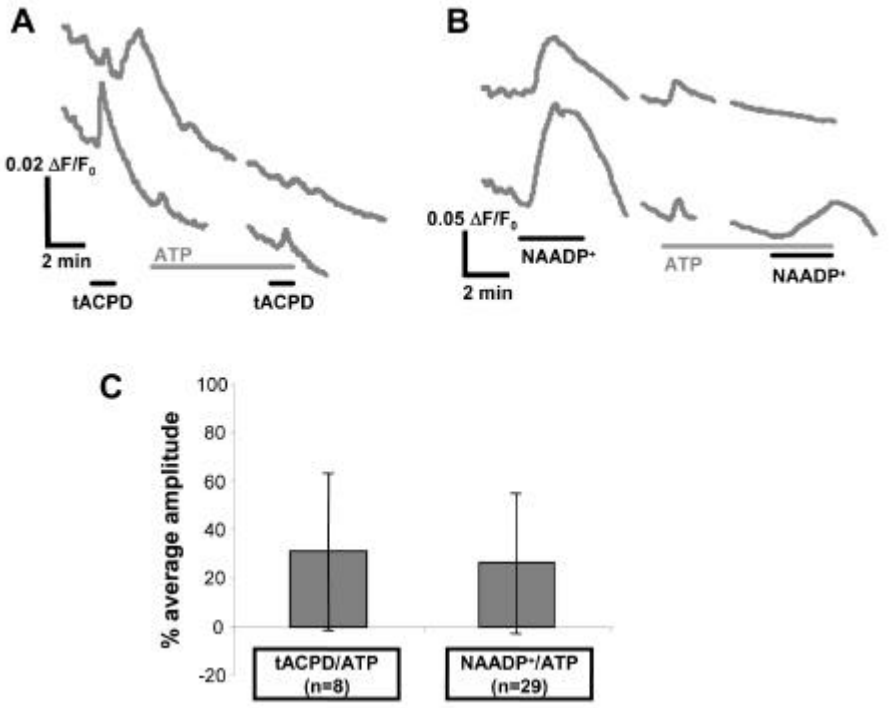

Fig. 13 Possible contribution of the purinergic pathway

A, two average F/F_0 traces calculated from all responsive cells of one slice representing the strongest and the weakest reduction of a tACPD-initiated response in the presence of ATP (100 µM, 3-5-min preincubation) in comparison with a first control response to tACPD (50 µM) are shown. *B*, as in *A*, two average F/F_0 traces are shown to demonstrate the most and the least strongly reduced second reaction to $NAADP^+$ in the presence of ATP in comparison with a first control reaction to $NAADP^+$. *C*, the graph shows percentages of maximal F/F_0 amplitudes of average traces in response to tACPD or $NAADP^+$ application in the presence of ATP compared to a control condition (equal to 100%). The numbers of slices (*n*) averaged are given in the figure.

The generic adenosine receptor inhibitor CGS-15943 (10 μM) effectively reduced adenosine (10 μM)-induced Ca^{2+} signals in astrocytes in brain slices (*n* = 7; Fig. 14, *A* and *C*). In comparison with control application of $NAADP^+$ and after a 10-minute washout, which included a 7–8-minute preincubation with CGS-15943, CGS-15943 had a similar effect on $NAADP^+$-induced signaling (*n* = 17; Fig. 14, *B* and *C*).

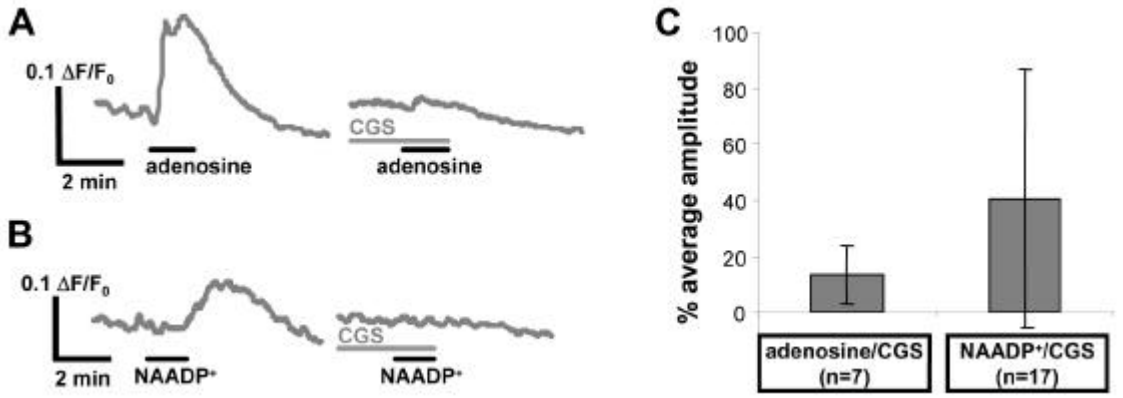

Fig. 14 Adenosine receptor-mediated contribution

A, the trace represents an average F/F_0 trace of all reacting cells in one slice showing a first reaction to adenosine (10 μM) and a second adenosine application in the presence of CGS-15943 (10 μM, 7-8-min preincubation). *B*, average F/F_0 trace of all reacting cells in one slice showing an example of a first reaction to $NAADP^+$ and a second reaction to $NAADP^+$ in the presence of CGS-15943. *C*, the *graph* shows percentages of maximal F/F_0 amplitudes of average traces in response to adenosine or $NAADP^+$ application in the presence of CGS-15943 compared with a control condition (equal to 100%). The numbers of slices averaged are given in the figure.

3.1.9 Astrocytes and neurons expressed the $NAADP^+$-synthesizing enzyme CD38 *in situ*

To gain information about the distribution of the $NAADP^+$ synthesizing enzyme CD38, a specific antibody to CD38 was used to immunolabel neocortical cryosections (16 μm) of 2-week-old mice. To identify astrocytes, they were double-labeled with an antibody against the astrocyte-specific marker S-100β (secondary antibody coupled to Cy2; Fig. 15*a*). Neurons were identified based on their morphology.

Both neurons and a subset of astrocytes in the neocortex, were labeled by the antibody against CD38 (Fig. 15*b*). In the image overlays (Fig. 15*c*), the *arrows* indicate double-labeled astrocytes.

The neuronal staining for CD38 was much stronger than that of astrocytes, and the neuronal staining was especially prominent in the perinuclear region. The astrocytic staining was much weaker, more diffuse, and found in processes rather than in the cell body.

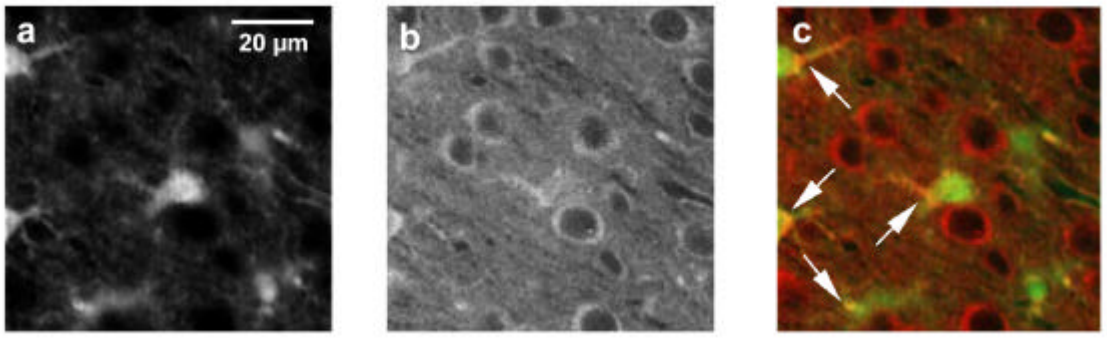

Fig. 15 Astrocytes and neurons expressed the NAADP$^+$-synthesizing enzyme CD38 *in situ*

Neocortical cryosection (16 mm, 2 weeks) double-immunostained for the astrocytic marker S-100β (secondary antibody coupled to Cy2, *green*; (*a*)) and for CD38 (secondary antibody coupled to Alexa-594 nm, *red*; (*b*)). Neocortical neurons and subsets of astrocytes (*green*) express CD38 (*red*), seen in the image overlays. The *arrows* point to double-labeled astrocytes (*c*).

3.1.10 NAADP$^+$ triggered Ca^{2+} signaling in cultured neurons and glial cells

Finally, the ability of NAADP$^+$ to trigger Ca^{2+} signals in neurons and other glial cell types was investigated. Cultured neurons from cerebellum (predominantly granule cells; n = 11 coverslips), cortical oligodendrocytes (n = 7 coverslips), and microglial cells (n = 3 coverslips) were loaded with the Ca^{2+}-sensing dye Fluo-4/AM. Application of NAADP$^+$ (5 or 10 µM, 2–3 minutes) triggered transient intracellular Ca^{2+} increases in all cell types studied (Fig. 16).

However, not all cells tested react to NAADP$^+$; the glioma cell line GL261 did not react to NAADP$^+$ stimulation (n = 7 coverslips, data not shown); nor did the 1321N1 human astrocytoma cell line (n = 4 coverslips, data not shown).

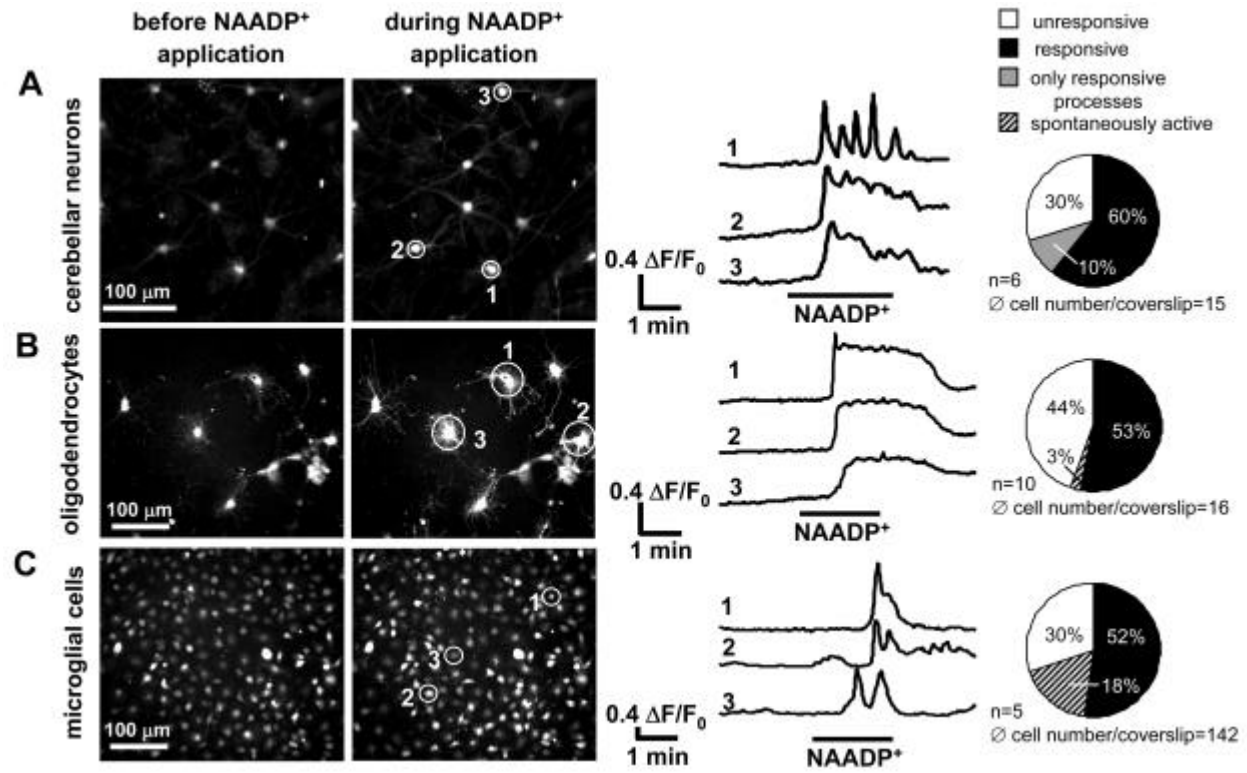

Fig. 16 NAADP$^+$ triggered Ca^{2+} signaling in cultured neurons, oligodendrocytes, and microglial cells

Fluorescence images of Fluo-4-loaded cultured cerebellar neurons (*A*), oligodendrocytes (*B*), and microglial cells (*C*) are displayed before and during NAADP$^+$ application (5 µM for neurons, 10 µM for oligodendrocytes and microglia). In the *middle*, fluorescence recordings (F/F_0) are displayed from the cells marked by *circles* in the fluorescence images. On the *left*, percentages of responding, spontaneously active, and unresponsive cells are indicated in *pie diagrams*.

3.2 Stop of perfusion-induced Ca^{2+} signaling

3.2.1 Switching off the perfusion induced different types of Ca^{2+} responses in astrocytes in acute cortical brain slices

During the process of carrying out the above measurements, it was noted that upon switching off the perfusion, an increase in Ca^{2+} signaling was induced in astrocytes in acute cortical brain slices. This has previously been observed in this group by Peters et al. [285]. The signaling activity normalized, when the superfusion was turned on again (Fig. 17). The time from switching off the superfusion to the onset of the reaction (flowrate 3-4 ml/min, chamber volume

~1-1.5 ml) took on average 30 seconds. After switching the perfusion back on, the induced signaling ceased rapidly. During the period of 3-4 minutes, in which the perfusion was switched off, different types of Ca^{2+} responses, even within the same slice, were evoked, including single peak responses, oscillations, oscillations superimposed on a transient Ca^{2+} increase, elevated plateaus, as well as oscillations followed by elevated plateaus, and plateaus with superimposed oscillations. The oscillations had a frequency of 2-4 oscillations per minute. Usually responses persisted during the recording time.

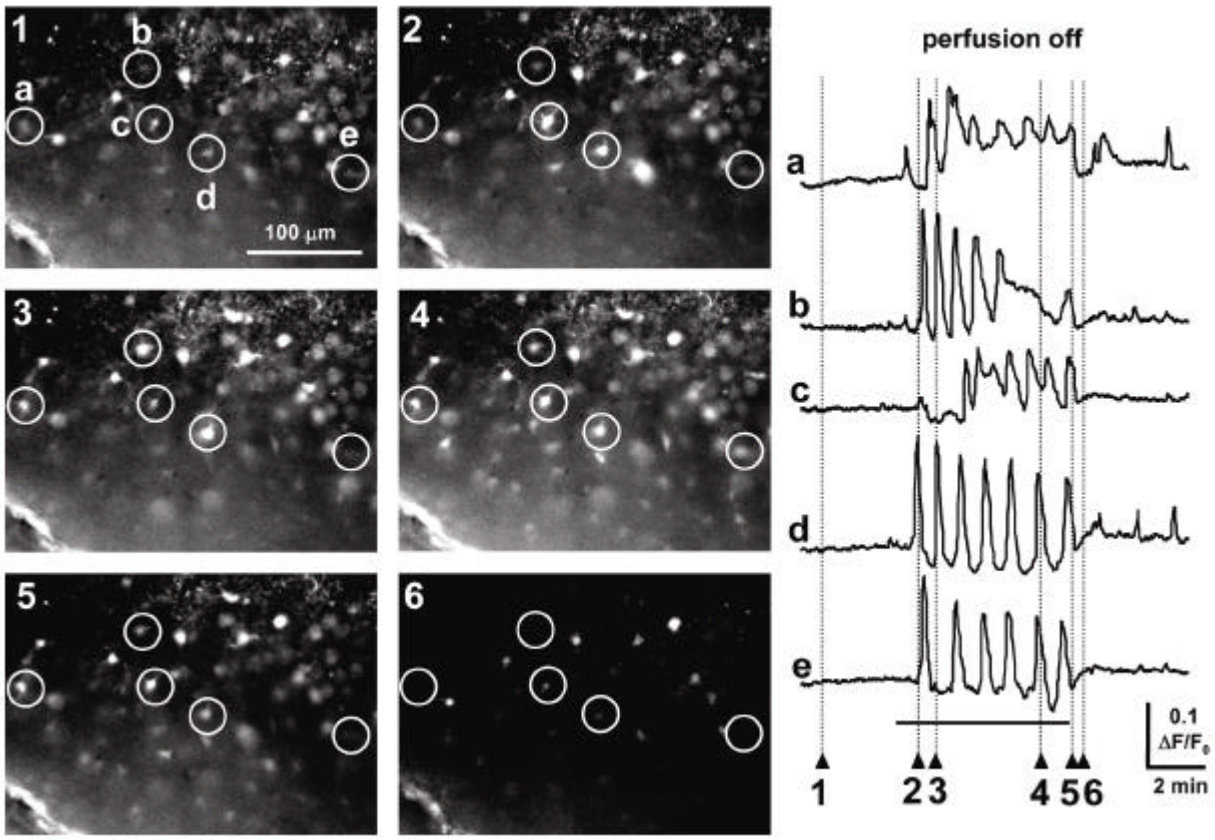

Fig. 17 Switching off the perfusion induced different types of Ca^{2+} responses in astrocytes in acute brain slices
A, astrocytes in a neocortical slice stained with the Ca^{2+}-sensitive dye Fluo-4. The *fluorescence images* are taken before and at different time points during and after switched off perfusion. Circles label 5 cells, which exhibit an increase in Fluo-4 fluorescence, and their corresponding F/F_0 traces are shown below in *B*. The time points at which the images were taken, are marked by numbered triangles below the traces. The period during which the perfusion was switched off is indicated by a black line below the traces here and in all following figures. Note that responses can be diverse among different cells within one slice.

3.2.2 Switching off the perfusion can repeatedly evoke Ca^{2+} responses in astrocytes

The response within a selected cell was largely reproducible when the perfusion was switched off a second time after a 5-15-minute long superfusion period. The responses were similar for individual cells following the first and second switch-off of the perfusion (Fig. 18*B*). Average responses for a given slice were also comparable for a first and a second switch-off of the perfusion (Fig. 18*A*).

In terms of cell numbers, 89 ± 14% of the cells, which had reacted during the first stop of perfusion period, reacted again during the second. Activity was evoked in some additional cells during the second trial, but their number was with 16 ± 38% very variable (*n* = 12, ∅ cell number/slice = 31 ± 19; Fig. 18*D*). As a measure of amplitude and oscillatory behavior of the Ca^{2+} signals, the "overall average amplitude change" (for details, see Material and Methods 2.6.2) was calculated for the periods before, during, and after switched off perfusion. In this manner an activity profile was obtained, in which the activity value for the first stop of perfusion period was set at 100%.

The basal level "overall average amplitude change" value before switching off the perfusion the first time was 33 ± 15%. Upon switching on the perfusion, it returned to 39 ± 11% (*n* = 4, ∅ cell number/slice = 41 ± 17; Fig. 18*C*). The difference between basal activity and switch-off of the perfusion-induced activity may be underestimated, as many cells reached Ca^{2+} plateaus and therefore did not further contribute to the average amplitude change value, even though their Ca^{2+} levels were still elevated. The average amplitude change during the second stop of perfusion was only 66 ± 14% of that during the first, but was still significantly higher than the basal level average amplitude value (34 ± 10%; Fig. 18*C*) before the perfusion was switched off.

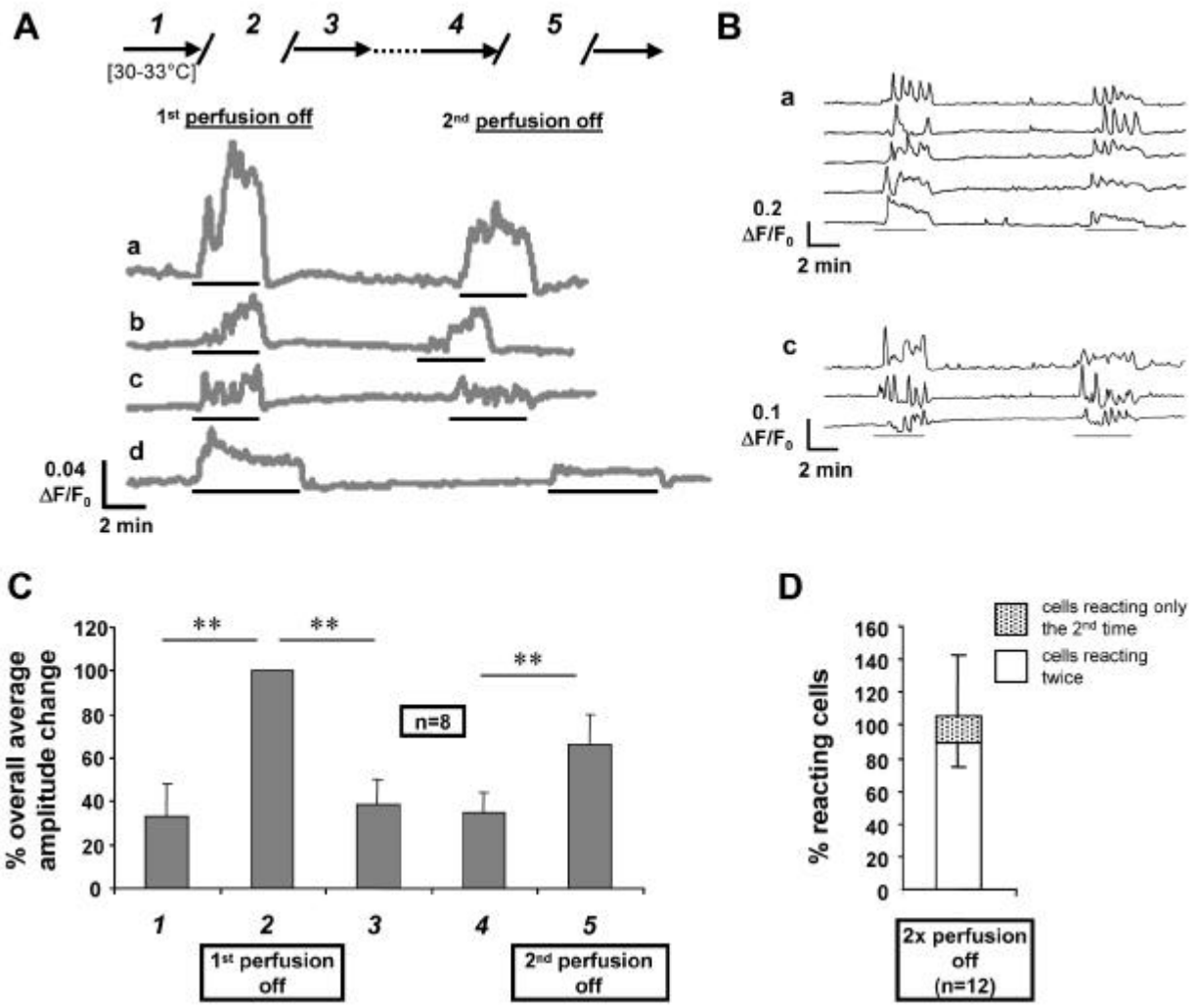

Fig. 18 Switching off the perfusion can repeatedly evoke Ca^{2+} responses in astrocytes

A, average F/F_0 traces (*gray*) are shown for four experiments (*a-d*) in which the perfusion was switched off consecutively two times, according to the general *scheme above*. Comparable activity was induced both times. *B*, representative F/F_0 traces of single cells (*black*) from experiments *A*(*a*) and *A*(*c*). *C*, The *bar diagram* shows the "average activity profile" for eight experiments. The "overall average amplitude change" for all cells was calculated for time windows before, during and after switched off perfusion as indicated by *numbers 1-5* in the *scheme* in *A*. The *activity profile* reflects higher activity during the two times of switched off perfusion in contrast to times with running perfusion. In *D*, the numbers of astrocytes responding during the two subsequent times of switched off perfusion are compared. It is subdivided into cells, which reacted both times and cells, which reacted only during the second one. Almost all cells, which had reacted a first time, reacted again. *, $p < 0.05$; **, $p < 0.005$.

3.2.3 Switching off the perfusion is accompanied by a drop in temperature, which is the major trigger of the observed Ca^{2+} signalling

Measuring with bicarbonate buffer heated to 30-33°C, an average drop of ~7°C to room temperature (~22-24°C) was detected in the recording chamber within ~4 minutes, with a drop of temperature of 3°C occurring within the first minute (*n* = 17; Fig. 19). This was due to the fact that only the inflow tubing and not the chamber was heated.

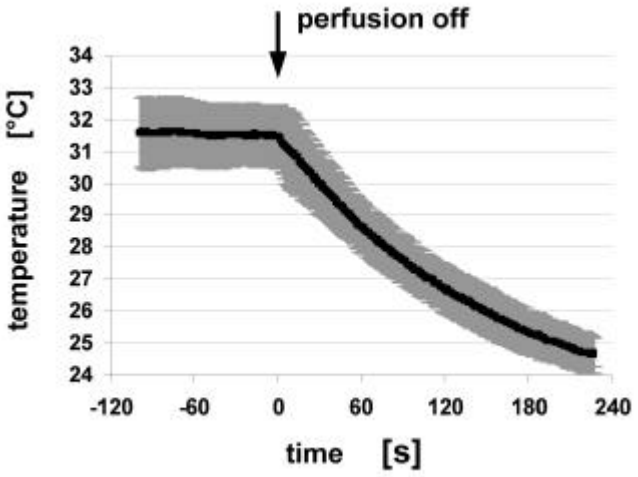

Fig. 19 Drop in temperature during switched off perfusion

The graph shows the drop in temperature measured in the microscope chamber during recordings, in which the perfusion was switched off. The *black* trace is an average of 17 experiments; *gray* are the error bars (standard deviation). The time point of the stop of the perfusion is 0.

Consequently, it was investigated whether the induction of Ca^{2+} oscillations in astrocytes was temperature-dependent. Indeed, turning off the heating of the buffer inflow induced Ca^{2+} signaling in astrocytes very similarly to turning off the perfusion. When a first recording period, during which the perfusion was switched off, was compared to a second, during which the heating was turned off, Ca^{2+} responses were very similar. Single cell (Fig. 20*B*) and average (Fig. 20*A*) F/F_0 traces reflected this similarity where 99 ± 2% of the cells were stimulated from both stimuli (*n* = 4, ∅ cell number/slice= 42 ± 11; Fig. 20*D*). The overall average amplitude change caused by turning the heating off was also very similar (102 ± 40%; Fig. 20*C*) to the one caused by switching off the perfusion.

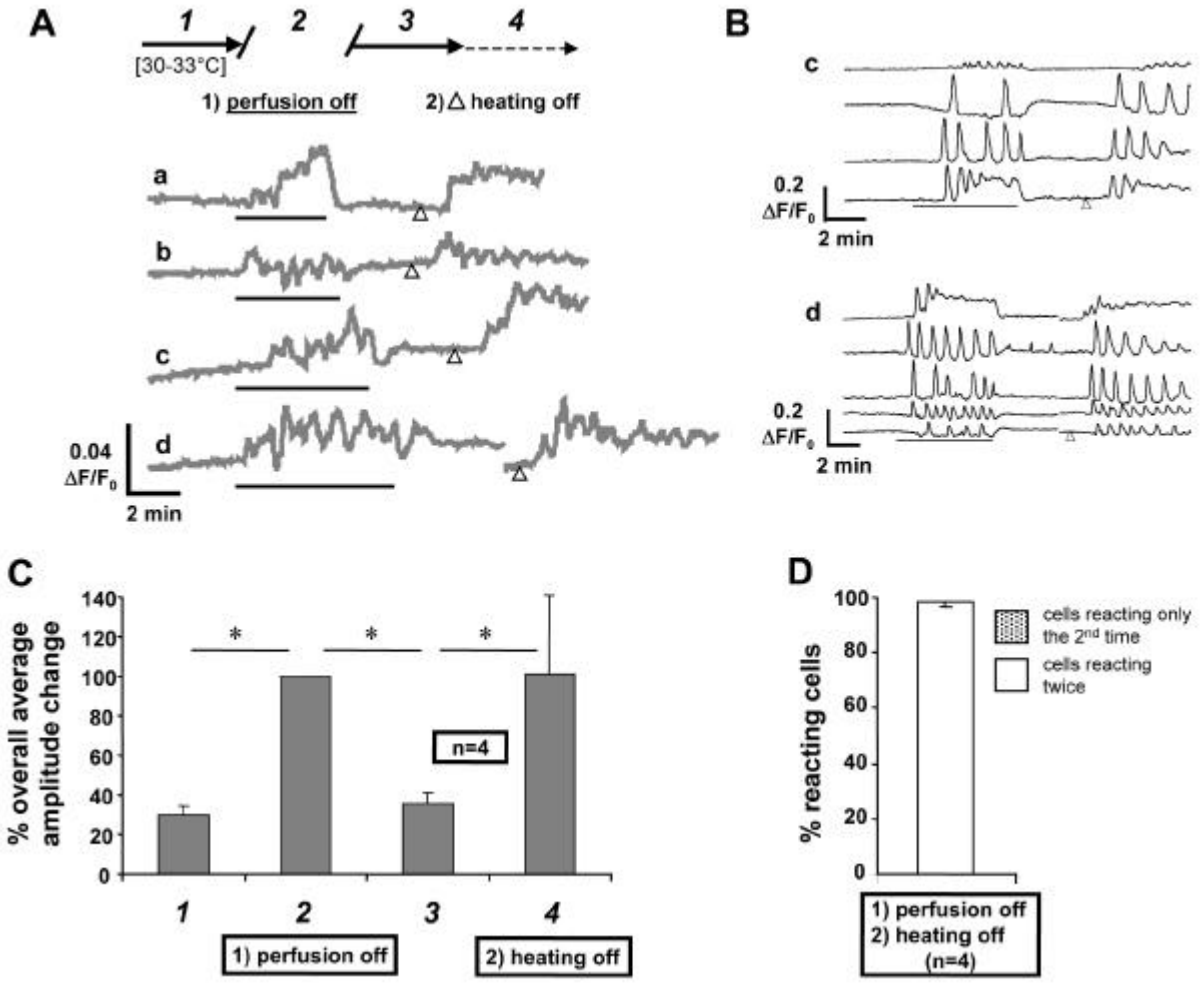

Fig. 20 Switching the heating off mimics the Ca^{2+} signaling induced by switching off the perfusion

A, average F/F_0 traces of four different experiments are shown for experiments, in which the perfusion was switched off first (*black bar*), and subsequently the heating was switched off (*white triangle*) according to the general *scheme above*. Both paradigms induced similar activity. *B*, representative F/F_0 traces of single cells from experiment *A*(*c*) and *A*(*d*). *C*, The "*average activity profile*" reflects higher activity during the time windows (indicated by *numbers 1-4* in the scheme in *A*) where the perfusion or heating was switched off (windows *2* or *4*). The activity is comparable in both cases (*C*, *2* and *4*) as is the population of cells (*D*). *, $p < 0.05$; **, $p < 0.005$.

To evaluate whether other factors apart from the decrease in temperature contributed to the signaling during switched off perfusion, the measuring chamber was heated to maintain a constant temperature, while the perfusion was switched off. In this case, the number of reacting cells was significantly reduced to 33 ± 27% of the number of cells active during a subsequent period of switching the perfusion off, when the chamber was not heated ($p < 0.05$; $n = 12$, ∅ cell

number/slice = 31 ± 14; Fig. 21*A*). Of these residual cells 28 ± 22% reacted during both periods, whereas 5 ± 8% reacted only when the chamber was heated. In some average F/F_0 traces, a small residual increase in activity, even during switched off perfusion at stable temperature, could be visualized (Fig. 21*B*).

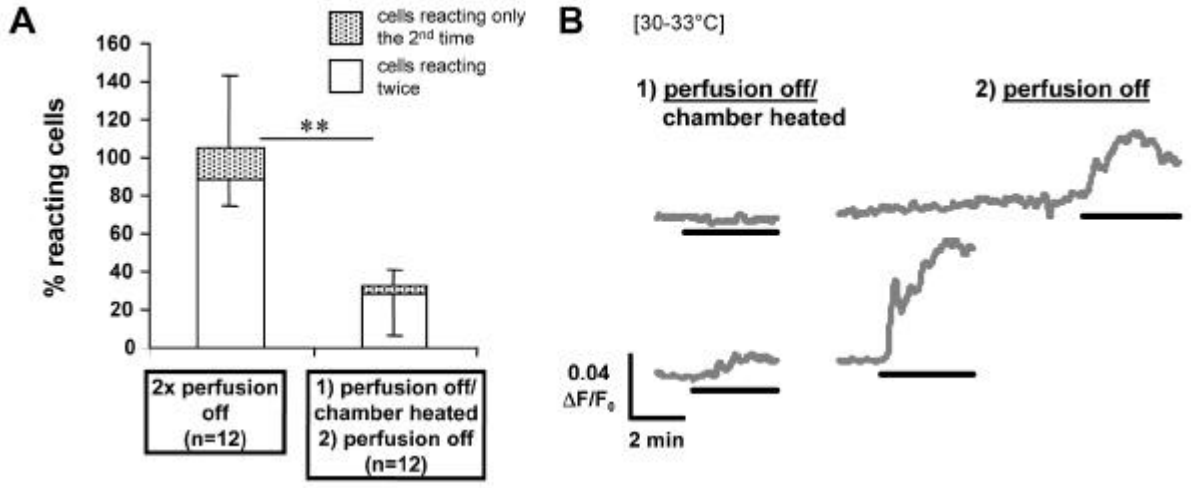

Fig. 21 The drop in temperature mainly accounts for the signaling induced by switching off the perfusion

A, bar graph showing the number of cells reacting when the perfusion was switched off, while the measuring chamber was kept at steady temperature (30-33°C) independently of the inflow. The *first bar* represents the control situation, in which the perfusion was switched off two times without heating the chamber (see Fig. 18*D*). The *second bar* demonstrates that significantly less astrocytes responded to switched off perfusion when the chamber was heated than when it was not. *B*, F/F_0 average amplitude traces of two representative experiments. *, $p < 0.05$; **, $p < 0.005$.

3.2.4 Basal Ca^{2+} signaling activity in cortical astrocytes is higher at RT than at higher temperatures (30-33°C or 37-38°C)

However, a slight residual drop in temperature accounting for the remaining signaling could not be excluded. Therefore, to keep a stable temperature, the effect of switching the perfusion off was investigated at room temperature (RT, ~22-24°C). When recording basal level activity at room temperature, generally more cells were active than at higher temperature (30-33°C). Ca^{2+} signaling activity was frequently observed throughout the whole first part of the experiment, therefore interfering with the measurement (Fig. 22, *B* and *D*(*d*, *e*), Fig. 23*D*(*b*), and Fig. 24*D*(*b*)). Due to this high basal activity, the chosen method of analysis of counting active cells was not practicable any more. Inferred from average F/F_0 traces, switching off the perfusion at

RT alone seemed to induce Ca^{2+} signaling activity of cells (Fig. 22, *A* and *B*), although, taking a closer look, activity had already begun to rise before switching off the perfusion. The signaling patterns of single cells were diverse: cells could remain unaffected, active cells could alter their oscillatory pattern with regard to frequency or amplitude, oscillations could turn into plateaus, silent cells could be activated, and active cells could become inactive (Fig. 22*B*). After switching the superfusion on again, the activity did not stop abruptly in most instances, but continued and declined only gradually (Fig. 22, *A* and *B*). The effects evoked by turning the superfusion off at RT could not be elicited a second time within the same slice. Regarding average F/F_0 traces, switching off the perfusion a second time appeared to induce activity slightly (Fig. 22*A*). However, since the majority of cells were quiescent in the second part of the recording, the average traces were strongly affected by Ca^{2+} level raises of isolated cells (Fig. 22*B*). This is well illustrated with the experiment (*a*) in figure 22 *A* and *B* (*third cell from top*).

As reported above, many cells were already or became active within the first few minutes of a basal level recording at RT with the perfusion switched on. Activity patterns throughout these recordings at RT were similar to those in measurements, during which the perfusion was switched off at RT (Fig. 22, *C*(*d*, *e*) and *D*(*d*, *e*)). This alone might account for the rise in activity observed in the latter case. At higher temperatures, the basal activity did not increase during experiments (for 30-33°C see Fig. 18, *A* and *B*, and Fig. 20, *A* and *B*; for 37-38°C see Fig. 22, *C*(*f*, *g*) and *D*(*f*, *g*)).

The high signaling activity observed at RT could be suppressed by raising the temperature to 30-33°C (Fig. 23). When the heating was turned on during a recording, the overall average amplitude change decreased to 65 ± 18% (n = 3, ∅ cell number/slice = 35 ± 15; Fig. 23, *C* and *D*). Activity could be restored again (154 ± 70%) by switching the heating off and thereby lowering the temperature back to RT. In an analogous set of experiments the by an elevation of temperature reduced activity (49 ± 14%, $p < 0.05$; n = 3, ∅ cell number/slice = 37 ± 18; Fig. 23, *A* and *B*) could be similarly restored (92 ± 16%, $p < 0.05$) through lowering the temperature by turning the perfusion off. Overall average amplitude change values were consistently lower at 30-33°C than at RT before and afterwards within the same slice, but the variation between different slices was relatively high. Therefore, the number of experiments was too low to reach significance in all cases.

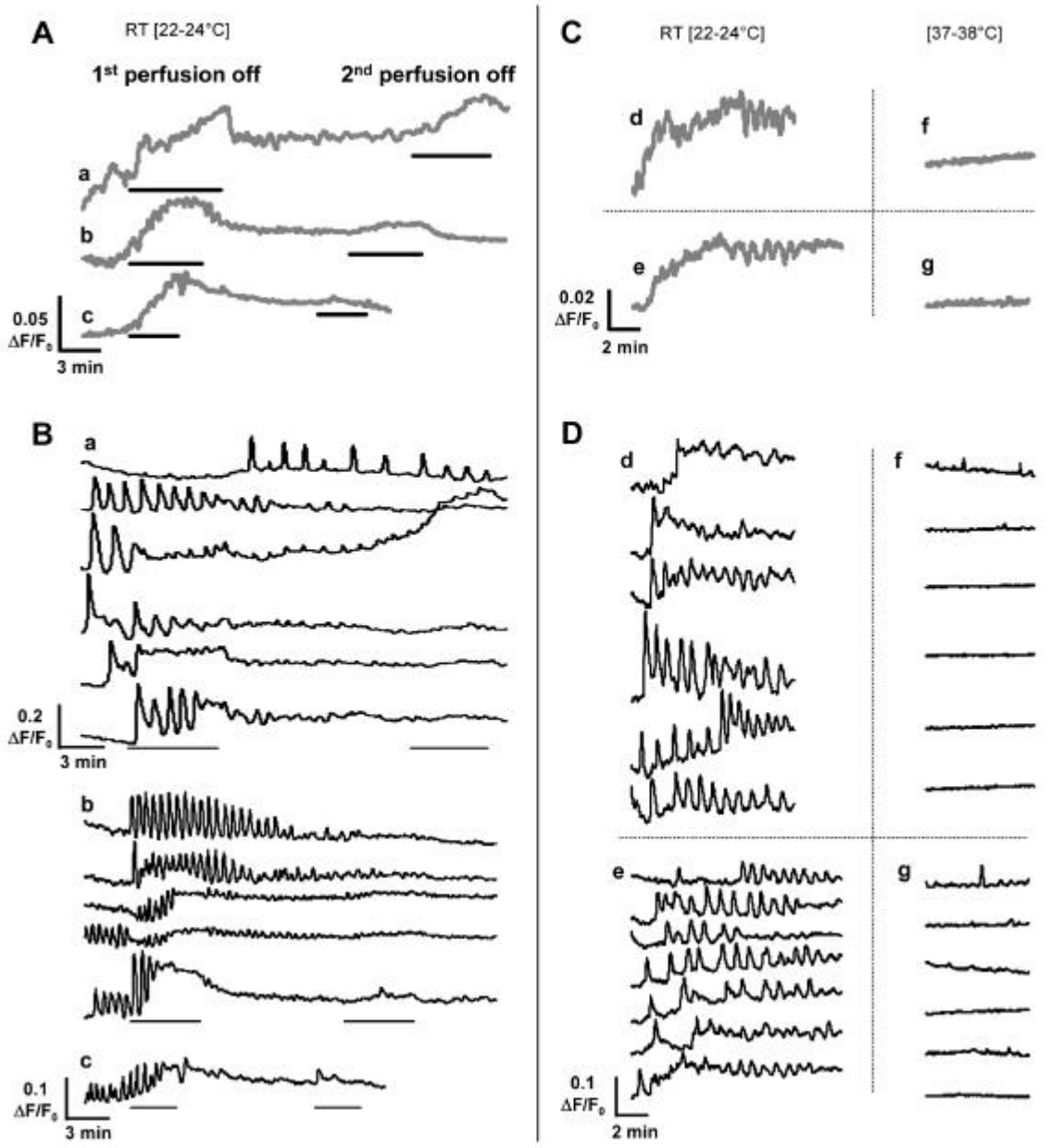

Fig. 22 At room temperature switching off the perfusion does not induce activity and basal activity is higher than at higher temperature (37-38°C)

A, average F/F_0 traces of three experiments in which the perfusion was switched off twice at RT. Note that the rise starts already before switching off the perfusion and that the effect cannot be evoked a second time to a similar extent. *B*, F/F_0 traces of single cells from the respective experiments (*a*, *b*, *c*) shown in *A*. It becomes clear that many cells were already active before switching the perfusion off the first time and that very few cells account for the minor rise in the average traces during the second switch-off. *C*, average F/F_0 traces of two basal level measurements during perfusion at RT (*d*, *e*) and other two at 37-38°C (*f*, *g*). *D*, single cell F/F_0 traces of the respective measurements at RT (*d*, *e*) and at 37-38°C (*f*, *g*).

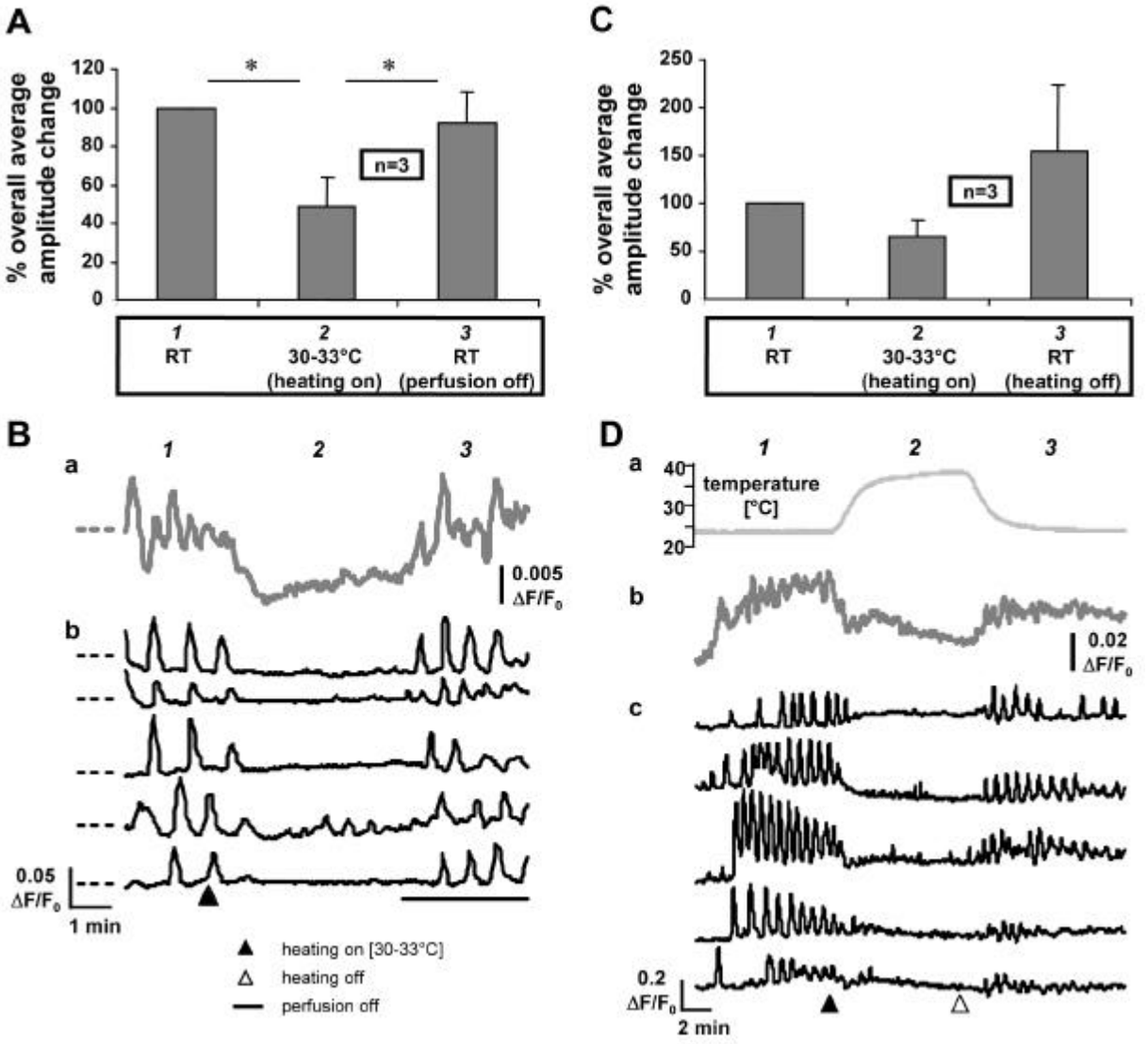

Fig. 23 Activity at room temperature is abolished by switching on the heating and can be recovered by switching the perfusion or heating off

A, the *average activity profile* reveals that activity is lower with the heating switched on to 30-33°C (period *2*) than at room temperature (activity at RT set 100% for *period 1*). The *third bar* in the *diagram* indicates a recovery of activity by switching off the perfusion (*3*). One representative average F/F_0 trace is shown in *B(a)* above single cell F/F_0 traces from the same experiment (*B(b)*). Accordingly, an average activity profile (*C)* and average (*D(b)*) and single cell traces (*D(c)*) are shown for a similar type of experiment in which the activity could be recovered by switching the heating off (*3*). In addition, the temperature measured in the recording chamber during this experiment is shown above the traces in *D*(*a*). *, $p < 0.05$; **, $p < 0.005$.

3.2.5 More cortical astrocytes exhibit Ca^{2+} signaling at 30-33°C than at 37-38°C

Measurements were initially conducted at 30-33°C, although not at the physiological temperature of 37-38°C [292], since tissue is more sensitive to cell death and dye leakage is prominent at higher temperatures. Nevertheless, in the next set of experiments, the Ca^{2+} signaling activity was recorded during lowering the temperature from 37-38°C to 31-34°C to examine the relevance of drop in temperature-induced astrocytic Ca^{2+} signaling for physiological temperatures. Mild hypothermia within this temperature range [293] is used clinically to attenuate further damage after brain injury [294-296].

Two sets of experiments were carried out, in which the induced activity by lowering the temperature from 37-38°C to 31-34°C was compared to the activity at RT. In the first set (Fig. 24, *A* and *B*), the temperature was decreased to 31-34°C by switching the perfusion off while heating the chamber to 31-34°C. This was followed by the drop in temperature from 37-38°C to RT, used as reference. For comparison, active cells were counted for the periods at 37-38°C, 31-34°C and RT and the number of cells active at RT was set at 100% (n = 6, ∅ cell number/slice= 43 ± 17; Fig. 24*A*). At 37-38°C, 18 ± 10% of the cells were active. At 31-34°C the number of cells exhibiting Ca^{2+} signaling doubled to 40 ± 20%.

In the other set (Fig. 24, *C* and *D*), the temperature was decreased by switching the inflow heating off for a short period, and the experimental order was reversed so that the reference period measured at RT was at the beginning of the experiment before it was heated up to 37-38°C. With 26 ± 16% the number of active cells was lowest at 37-38°C (Fig. 24*C*). At 31-34°C it was again roughly twice as high (47 ± 26%). In this case significance was not reached due to the low number of experiments (n = 4).

These results demonstrate that the induction of mild hypothermia by either, switching off the perfusion or the heating, had a comparable effect. Additionally, the experimental outcome was unaffected by the order of the period at RT and the decrease in temperature to mild hypothermia. In conclusion, the effect is of physiological relevance, however, not as prominent as in the lower temperature range. In any case, the findings have methodological implications. Therefore, the stop of perfusion/drop in temperature–induced signaling was continued to be investigated.

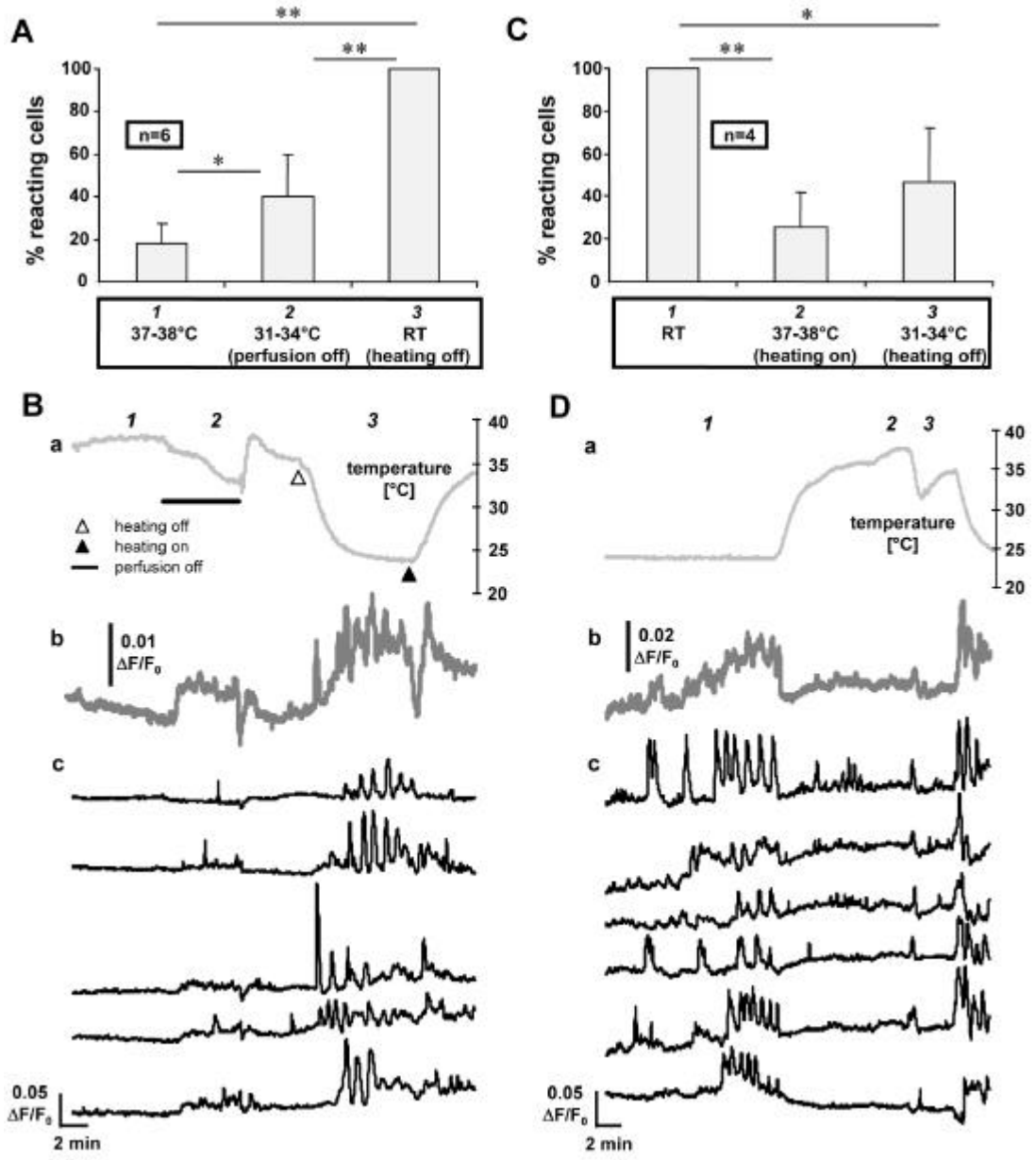

Fig. 24 Activity is higher at 31-34°C than at 37-38°C

A, active cells were counted at a period of 37-38°C (*first bar*), at a period during which the perfusion was switched off and the temperature decreased to 31-34°C as the chamber was heated (*second bar*), and a period in which the temperature dropped from 37-38°C to RT by turning the heating off (*third bar*, 100%). More cells were active at 31-34°C than at 37-38°C. The course of temperature during one experiments is shown in *B(a)* above the average F/F_0 trace (*B(b)*) and single cell F/F_0 traces of the same experiment (*B(c)*). Accordingly, active cell numbers (*C*), temperature (*D(a)*), and average (*D(b)*) and single cell F/F_0 traces (*D(c)*) are shown for a similar type of experiment on the right. Here the experiments were started at RT (*first bar*), then the heating was switched on to reach a stable level of 37-38°C (*second bar*) and then the temperature was lowered to 31-34°C by switching off the heating (*third bar*), *C*. *, $p < 0.05$; **, $p < 0.005$.

3.2.6 The observed Ca^{2+} signaling is mainly driven by Ca^{2+} influx

Pharmacological characterization was carried out at lower temperature (30-33°C), at which the effect of stopping the perfusion on astrocytic Ca^{2+} signaling was most prominent.

A first measurement was conducted to obtain an internal control value, before applying the respective pharmacological condition and switching the superfusion off a second time in the presence of the respective drug. All substances were washed in with the superfusion for 5 minutes after the control measurement if not stated otherwise. Cells reacting in the two conditions were counted.

First, it was evaluated whether the stop of perfusion/drop in temperature-induced astrocytic Ca^{2+} responses were due to Ca^{2+} influx from the extracellular space or due to Ca^{2+} released from intracellular stores. Therefore, Ca^{2+} was omitted in the perfusion buffer. The total number of responsive cells was slightly, but not significantly reduced to 78 ± 34% (n = 13, ∅ cell number/slice = 31 ± 15; Fig. 25*A*). Interestingly, only cells, which had reacted in control conditions, reacted under Ca^{2+}-free conditions. The experiment was repeated with the extracellular Ca^{2+}-chelator EGTA (1 mM) added to the Ca^{2+}-free buffer. This resulted in a highly significant reduction of the responsive cell number to 22 ± 11% of which were 1 ± 3% reacting additionally ($p < 0.005$; n = 8, ∅ cell number/slice = 31 ± 11; Fig. 25*A*). This procedure, however, could reduce the filling state of the intracellular Ca^{2+} stores, for which reason their integrity was tested with the metabotropic GluR group I agonists DHPG. Under the same conditions (nominally Ca^{2+}-free/EGTA) the reaction to DHPG (20 µM) was also significantly reduced, to 69 ± 30%, but not as strongly ($p < 0.05$; n = 11; ∅ cell number/slice = 46 ± 11; Fig. 25*B*). When DHPG was applied twice successively in standard bicarbonate buffer, interrupted by a 10-minute wash out, all cells reacted to both applications (n = 5, ∅ cell number per slice = 33 ± 8; Fig. 25*B*). For assessing the contribution of Ca^{2+} from intracellular stores to the signaling, a first control recording was compared to the second one after a 12-16-minute wash-in of thapsigargin. In the presence of thapsigargin (1 µM), less cells responded (75 ± 41%) with most of the cells (61 ± 33%) having reacted before and a few (14 ± 20%) reacting additionally (n = 10, ∅ cell number/slice = 39 ± 25; Fig. 25*A*). However, this reduction was not significant.

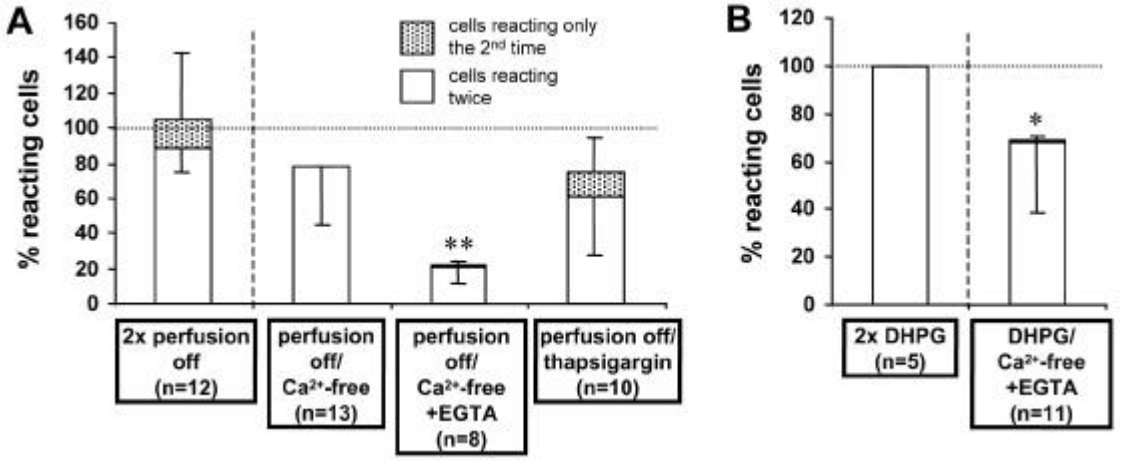

Fig. 25 The observed Ca^{2+} signaling is mainly driven by Ca^{2+} influx

A, the *first bar* (already shown in Fig. 18) shows the values obtained for control conditions. The *second* and *third bar* demonstrate the effects of 5-min preincubation with Ca^{2+}-free or Ca^{2+}-free/EGTA (1mM) buffer respectively. Under both conditions the number of active cells was reduced, although significantly only in the presence of EGTA. Control experiments for the integrity of internal stores under these conditions are shown in *B*. In Ca^{2+}-free/EGTA buffer less cells reacted to 20 μM DHPG (*B*, *second bar*), but this effect was not as pronounced as for switching the perfusion off. When the perfusion was switched off after a 12-16-min preincubation with thapsigargin (1 μM), the number of reacting cells was only slightly, however not significantly reduced (*A*, *fourth bar*). *, $p < 0.05$; **, $p < 0.005$.

3.2.7 Cellular swelling is involved in switching off the perfusion-evoked Ca^{2+} signaling

It was found that glioma cells and primary cultured astrocytes are swelling during hypothermia, less during mild (32°C) and more during moderate hypothermia (27°C) [73-75]. In turn swelling and mechanical stimuli in general are known to evoke Ca^{2+} responses in astrocytes (see Introduction 1.1.2). Above it was demonstrated that the signaling induced by switching off the perfusion is mainly due to a reduction of temperature. Therefore, swelling of astrocytes could occur and contribute to the hypothermia-induced Ca^{2+} signaling. Mannitol is used for preincubation of brain slices to suppress swelling during drug application [165;297]. Another application is its use in anesthesia and critical care medicine to reduce brain edema [296;298-300]. For these reasons the effect of hyperosmolar mannitol (100 mM) on the drop in temperature-induced Ca^{2+} elevations was investigated. The wash-in of mannitol itself caused Ca^{2+} responses similar to the stop of perfusion-induced signaling (Fig. 26, *A* and *B*). When the

Ca^{2+} reaction to switching off the perfusion was compared with the response to a subsequent mannitol administration, 74 ± 24% of the reacting cells were the same and 1 ± 2% reacted only to mannitol (*n* = 18, ∅ cell number/slice = 35 ± 17; Fig. 26*D*). The intracellular Ca^{2+} levels remained high for as long as mannitol was present. When the perfusion was switched off in the presence of mannitol, the intracellular Ca^{2+} levels rose further in the majority of cells, but oscillations were never observed (Fig. 26, *A*, *B* and *C*).

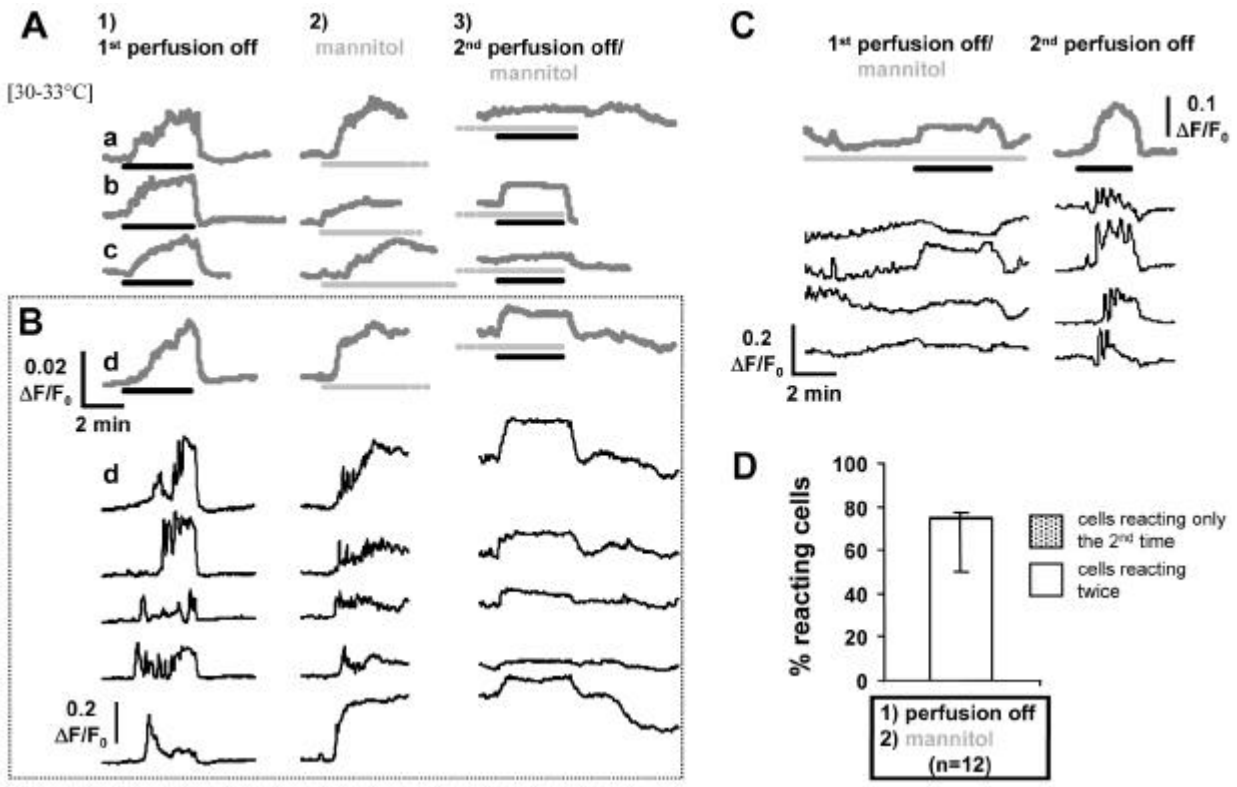

Fig. 26 Mannitol induces Ca^{2+} signaling and prevents oscillation after switching off the perfusion

A, three average F/F_0 traces of experiments where mannitol (2 mM) was applied for 5 min (*gray bars*) and then the perfusion was switched off (*black bars*) a second time in the presence of mannitol are shown. *B* shows an average trace above single cell F/F_0 traces of the same experiment. From the traces is evident that mannitol itself induced oscillatory Ca^{2+} signaling and rises Ca^{2+} levels. When the perfusion was switched off in the presence of mannitol, Ca^{2+} levels still rose, but oscillations were suppressed. *C*, the same effect, was observed, when the order of mannitol and control recording was reversed as seen in average and single F/F_0 traces. *D, bar graph* comparing the populations of activated cells by switching off the perfusion and by application of mannitol itself, which was largely overlapping.

3.2.8 Neuronal activity, connexin channels, glutamate, ATP, adenosine, and GABA do not contribute to the Ca^{2+} signaling

The drop in temperature and the associated swelling of the tissue could result in the release of substances acting on neurons and astrocytes by several mechanisms.

The influence of neuronal activity upon the astrocytic Ca^{2+} signals was investigated by application of tetrodotoxin (TTX), which inhibits voltage-gated sodium channels. In the presence of TTX (1 μM), Ca^{2+} signals were induced in 67 ± 12% of the cells, which had reacted in the internal control recording (n = 6, ∅ cell number/slice = 19 ± 16; Fig. 27). However, 15 ± 22% of cells reacted additionally so that the total number of responsive cells was 82 ± 30 % and therefore not significantly lower.

Next, it was tested, whether the perfusion-stop-induced astrocytic Ca^{2+} signals were affected by the block of connexin channels. Apart from a potential mechanosensitive release of glutamate and ATP through connexin hemichannels [87-89], gap junctional communication is involved in propagating Ca^{2+} signals between astrocytes in some brain regions [164;214;215]. Gap junctions and connexin hemichannels were blocked by carbenoxolon (100 μM). In comparison with internal controls, the number of cells participating in the signaling under these conditions was higher, although not significantly (154 ± 66%; n = 4, ∅ cell number/slice = 23 ± 10; Fig. 27).

It was proceeded to investigate whether some substances known to be released after cell swelling and which are generally capable of evoking Ca^{2+} responses and oscillations in astrocytes, are involved in the observed signaling. Such substances include glutamate, purines, adenosine, γ-aminobutyric acid (GABA), and NO (see Introduction 1.1.2 and 1.3.1). Their contributions were tested by inhibiting their respective receptors or by blocking their synthesis. Antagonists for metabotropic glutamatergic (MCPG, 500 μM), purinergic (suramin, 100 μM and reactive blue, 30 μM) and adenosine receptors (CGS-15943, 10 μM) were used, moreover the GABA(A) receptor antagonist bicuculline (10 μM) was applied. The situation observed for the inhibition of metabotropic glutamatergic and purinergic as well as GABA(A) receptors was comparable. In all cases more cells reacted during the pharmacological condition than during the preceding internal controls (for MCPG 148 ± 74%; n = 10, ∅ cell number/slice = 37 ± 28; for suramine 159 ± 48 %; $p < 0.05$; n = 7, ∅ cell number/slice = 19 ± 10%; for reactive blue 153 ± 42%; $p < 0.05$; n = 6, ∅ cell number/slice = 13 ± 7; for bicuculline 135 ± 22%; $p < 0.05$; n = 7, ∅

cell number/slice = 28 ± 7; Fig. 27). The number of additionally reacting cells was very variable (69 ± 67% for MCPG; 77 ± 47% for suramine; 74 ± 40% for reactive blue; 43 ± 31% for bicuculline), therefore the significance was not reached for all conditions. After the block of adenosine receptors by CGS-15943 (10-12-min preincubation) the number of reacting cells was lower, but not significantly reduced (84 ± 17%; *n* = 7, ∅ cell number/slice = 56 ± 10; Fig. 27).

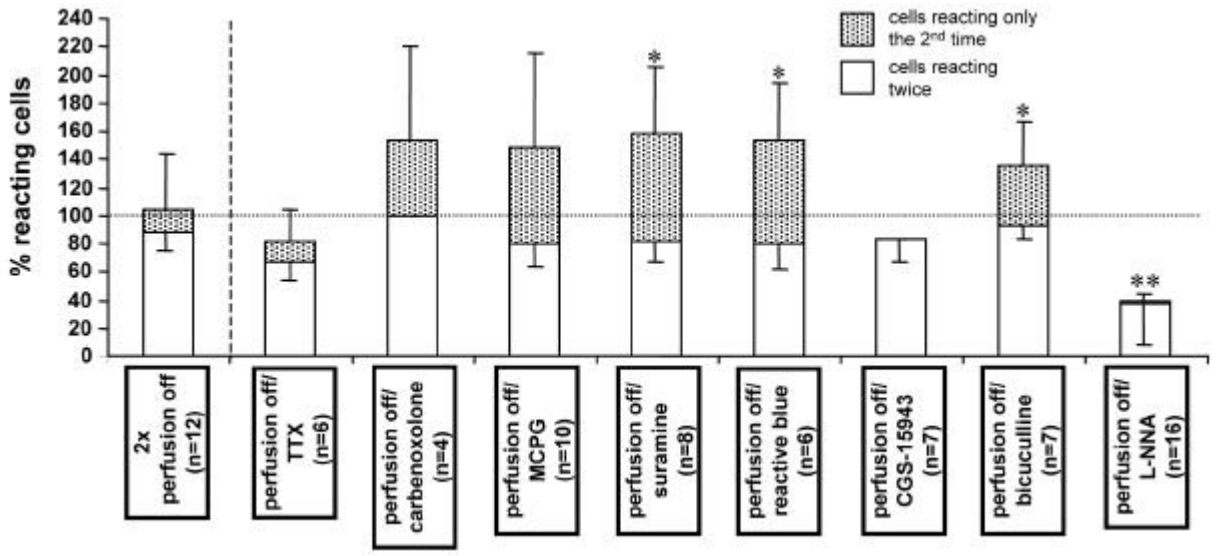

Fig. 27 Possible causes of the Ca^{2+} activity induced by switching off the perfusion – a role for NO

The *first bar* is already shown in Fig. 18*D*. The following *bars* illustrate in this order the effect on the number of reacting cells of 5-min preincubation with TTX (1 μM), carbenoxolone (100 μM), MCPG (500 μM), suramine (100 μM), reactive blue (30 μM), 10-12-min preincubation with CGS-15943 (10 μM), 10-min preincubation with bicuculline (10 μM), and finally 12-20-min preincubation with L-NNA (2 mM). TTX and CGS-15943 led to a slight, but insignificant reduction. Even though responses in the presence of carbenoxolone, MCPG, suramine, reactive blue and bicuculline are in average enhanced only the effect of both purinergic blockers was significant. L-NNA highly significantly reduced the activated cell number. *, $p < 0.05$; **, $p < 0.005$.

3.2.9 NO is involved in switching off of the perfusion-evoked Ca^{2+} signaling

As listed above, nitric oxide (NO) is another potential mediator of the observed Ca^{2+} responses in astrocytes, since NO-release is implicated in swelling- or stretch-induced as well as in astrocytic Ca^{2+} signaling (see Introduction 1.4.1 and 1.4.2).

After a 12-20-minute perfusion with the nitric oxide synthase inhibitor N_ω-nitro-L-arginine (L-NNA; 2 mM) the number of stop of perfusion-activated cells was significantly reduced when

compared to the internal control (39 ± 30%, $p < 0.005$; $n = 16$, ∅ cell number/slice = 32 ± 16; Fig. 27). 37 ± 28% had reacted before and only 2 ± 4% reacted additionally.

Prompted by the effect of NOS inhibition, the NO-donor S-nitrosoglutathione (SNOG; 100 µM) was applied to investigate whether NO could cause astrocytic Ca^{2+} signaling in acute cortical brain slices. SNOG induced reproducible oscillatory Ca^{2+} responses in cortical astrocytes (Fig. 28, *A* and *B*). During a second SNOG application the average total responding cell number was 97 ± 12% of that of a first administration, of which 93 ± 9% were the same cells ($n = 9$, ∅ cell number/slice = 31 ± 8; Fig. 28*C*). SNOG-induced Ca^{2+} signaling was then compared to switching-off the perfusion-induced signaling. A strongly overlapping population was activated by the two different stimuli. 83 ± 20% of the cells reacting to switching off the perfusion reacted as well to SNOG plus 5 ± 7 additional cells ($n = 5$, ∅ cell number/slice = 30 ± 13; Fig. 28*D*).

Results so far published regarding the pathway by which NO causes Ca^{2+} elevations in astrocytes in culture and other brain regions than the cortex are inconsistent. Here it was demonstrated for the first time that SNOG (NO) triggeres Ca^{2+} signaling in cortical astrocytes in acute brain slices. Therefore, it was continued to investigate the mechanism of NO-induced Ca^{2+} signaling in this preparation. After a first internal control application of SNOG, followed by a washout, it was applied a second time in Ca^{2+}-free buffer. Under nominally Ca^{2+}-free conditions, significantly less cells responded to SNOG than in the internal controls (59 ± 21%; $n = 8$, ∅ cell number/slice = 32 ± 15; Fig. 28*C*). For it has been stated that NO functions as a Ca^{2+}-influx factor responsible for SOCC-dependent refill of internal stores, the effect of blocking SOCCs by La^{3+} on the SNOG-evoked Ca^{2+} signaling was examined. In the presence of La^{3+} (20 µM), the number of reacting cells was not influenced, when compared to control conditions (96 ± 19%; $n = 10$, ∅ cell number/slice = 20 ± 10; Fig. 28*C*). Moreover, the contribution of ER stores was examined. After incubation with thapsigargin (1 µM) for 12-16 minutes, the SNOG-elicited Ca^{2+} signaling was almost abolished. Only 3 ± 8 % of the cells, which had reacted in internal controls, and no additional cells still showed responses ($n = 7$, ∅ cell number/slice = 23 ± 16; Fig. 28*C*).

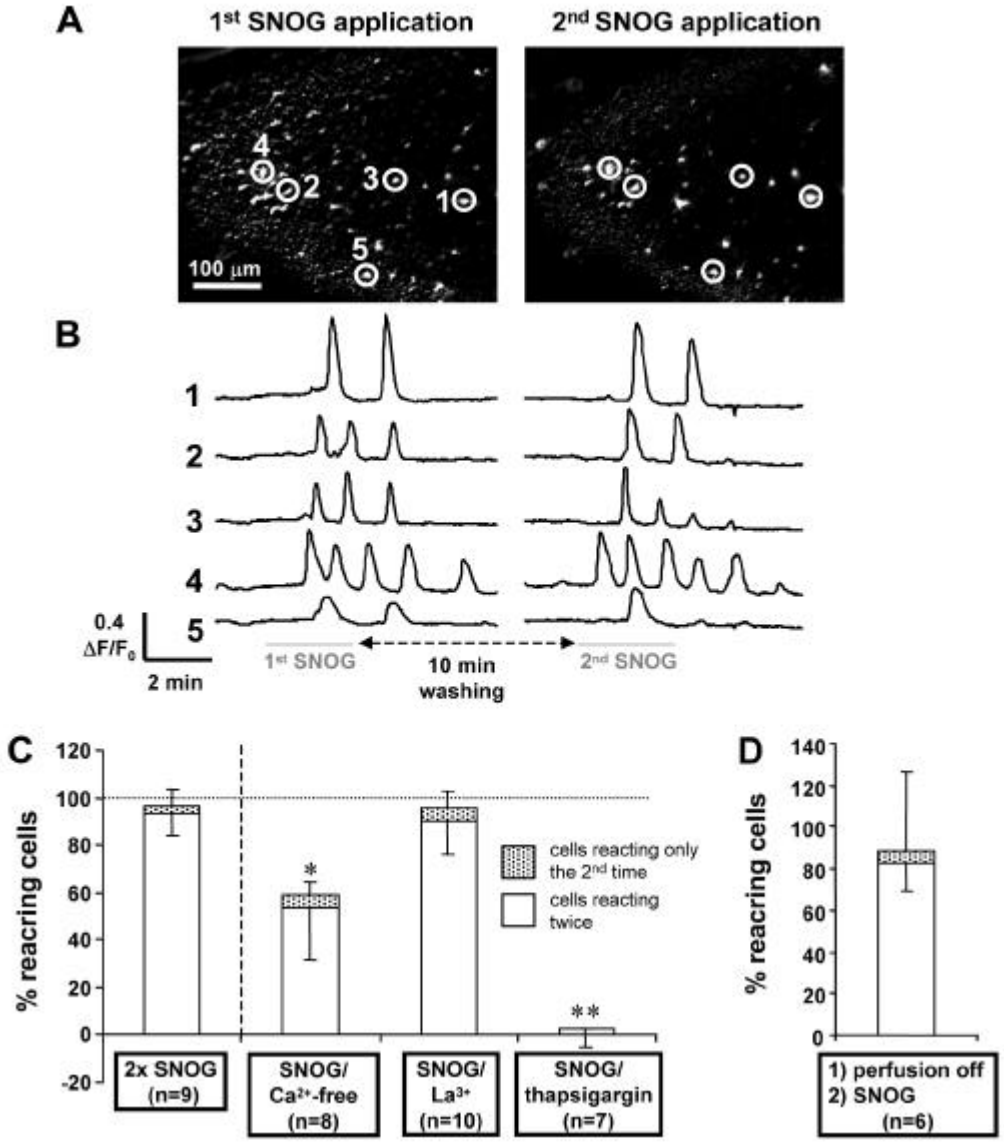

Fig. 28 The NO donor SNOG induces Ca^{2+} oscillations in astrocytes in acute brain slices

A, both *images* show reacting cells in the same neocortical region during two subsequent SNOG (100 µM) applications. *B*, F/F_0 traces from five cells of this experiment marked by circles in the images above. *C*, *bar graph* comparing the cell populations reacting to switching off the perfusion and reacting to SNOG, which are largely overlapping. *D, bar graph* comparing the numbers of cells reacting to a first SNOG application with those reacting to a subsequent second one under several pharmacological conditions. La^{3+} (200 µM) had no effect, Ca^{2+}-free buffer led to a significant reduction of the signaling; thapsigargin (1 µM) nearly abolished it. *, $p < 0.05$; **, $p < 0.005$.